THE MESSENGER

EL MENSAJERO

09. 09. 85
Munich

La Silla
La Serena
Santiago

No. 41 – September 1985

Comet Halley Observed at La Silla

While Periodic Comet Halley rapidly approaches the Sun, preparations are being made in many places to observe this distinguished celestial visitor. During most of the months of June and July 1985, Halley was "behind" the Sun and could not be observed. From about July 15, attempts to obtain images of Halley were made in various places, and it now appears that the first confirmed sighting was made at the European Southern Observatory on July 19.

On this date Halley was at declination +18 degrees and only 30 degrees west of the Sun. From the time the comet rose over the eastern horizon at La Silla to the moment when the sky brightness became excessive, there was at most 20 minutes. The only telescope at La Silla which is able to point in this direction is the 40 cm double astrograph (GPO) – all others are prohibited to do so by sophisticated computer control or limit switches without pity. The 40 cm is also the smallest telescope on La Silla, so the outcome of the attempt to observe Halley was very doubtful.

At this very low altitude, accurate guiding is difficult because the refraction in the Earth's atmosphere changes very rapidly as the object moves away from the horizon. Moreover, the expected brightness of Halley was only 14.5–15.0 and it could under no circumstances be seen in the guiding telescope. Offset guiding at the rate of the comet's motion was therefore necessary.

Together with Drs. Pereyra and Tucholke, I was not optimistic about the prospects on that morning, when we made the first attempt. A heavy bar which supports the dome obstructed the view and it was only possible to get one good 10-min. IIa-O plate. After processing, it was inspected carefully – it showed stars down to 16 mag or fainter, but there was no obvious comet image. Since the field is in the Milky Way, there were several very faint images; however, they all turned out to be faint stars when a comparison was made with the Palomar Atlas.

Another plate was obtained on July 20, but this morning the wind was strong and gusty and the telescope could not be held steady. The limiting magnitude was therefore about 0.5 mag brighter than on the preceding morning. Then came a snowstorm and with that the end of our attempts. We sent a telex to Dr. Brian Marsden at the IAU Central Telegram Bureau informing him about the negative result. The most important was of course that Halley appeared to be about 1.5 mag fainter than predicted.

Upon my return to ESO-Garching, by the end of July, ESO photographer C. Madsen and I decided to have a closer look at the plates. A photographically amplified copy was made of the July 19 plate (this method allows very faint, extended objects to be better seen), and the plate was measured in the S-3000 measuring machine. Indeed, a very faint, diffuse object was clearly seen near the expected position. It did not correspond

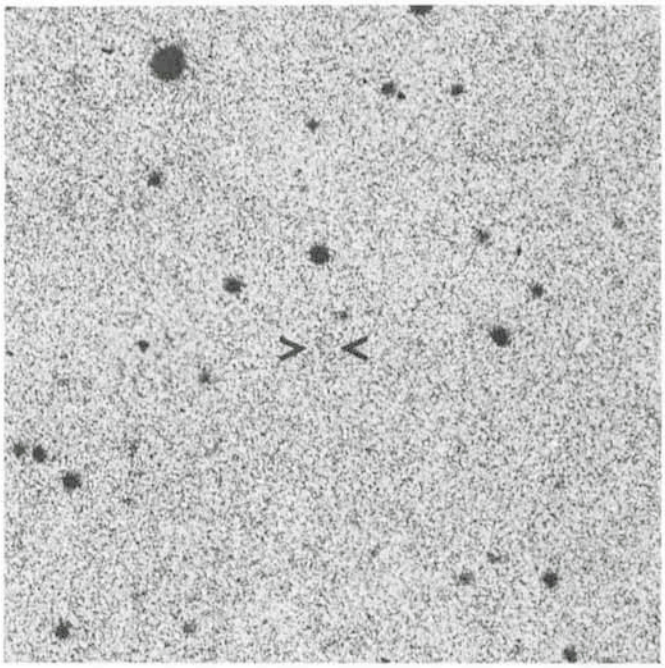

to any image on the Palomar Atlas. Although difficult to measure, a position could be transmitted to Dr. Marsden with the proviso that it would be wise to await confirming observations from other observatories before publication of the ESO position.

On July 27, 28 and 29 Halley was observed by Gibson at Palomar (60 inch telescope) and later, on August 1 and 4 by Seki in Japan. The magnitude of Halley on August 1 was 16, confirming our earlier estimate. These observations showed that our measurement on July 19 was within a few arcseconds of where Halley should have been, thus eliminating doubt about the correctness of the identification. The ESO observation was published on IAU circular 4090.

Although this fact in itself carries little scientific value, it bodes well for the ESO observations of Halley in mid-February 1986, when it reappears from behind the Sun, just after the perihelion passage. At that time our observations will be vastly more important, because they will contribute essentially to the navigation of the spacecraft, which are now en route to Halley for close encounters in early March 1986. And, of course, it is always nice to be the first, at least once in a while . . .!

R. WEST

The ESA PCD at the 2.2 m Telescope

S. di Serego Alighieri+, The Space Telescope European Coordinating Facility, European Southern Observatory*
S. D'Odorico, H. Dekker, B. Delabre, G. Huster, P. Sinclaire, European Southern Observatory
M.A.C. Perryman, M. Adriaens, ESTEC, Noordwijk
F. Macchetto, Space Telescope Science Institute, Baltimore*

The ESA PCD (Photon Counting Detector) (di Serego Alighieri et al., 1985a) was developed at ESTEC as a scientific model for the Faint Object Camera (FOC) of the Hubble Space Telescope (HST). It has been used at various telescopes (Asiago 1.8 m, ESO 3.6 m and 2.2 m, CFHT 3.6 m) providing us with data whose properties are very similar to those expected for FOC data (di Serego Alighieri et al., 1984 and 1985b). Since last April the PCD is offered to ESO visiting astronomers at the 2.2 m telescope within the terms of an ESA/ESO agreement, where ESA provides the detector and its computer system, the documentation and support during the first few times the instrument is operated at the telescope; ESO provides the interfaces for long slit spectroscopy and direct imaging, operational support, telescope time and data reduction software.

The PCD is a bidimensional photon counting detector consisting of a 3-stage image intensifier with magnetic focussing and bialkali first photocathode (Fig. 1), coupled by a reimaging lens to a television tube. The TV camera detects the scintillations at the output of the intensifier corresponding to the arrival of individual photons at the first photocathode. The central X-Y position of each burst is measured by a video processing electronics, and in an image memory the memory cell corresponding to that position is incremented by one. The image gradually builds up during the exposure and can be read non-destructively and displayed at any intermediate time. The detector and its electronics are controlled by a minicomputer, and the astronomer sits at a terminal in the control room. Displays are provided both for the analog output of the TV camera and for the digital data being integrated in the image memory. Experience has demonstrated that the possibility of easily and quickly monitoring the data, while these are acquired, considerably increases the efficiency and the quality of the observation. An IHAP station can also be used for the first data reduction at the telescope. The documentation available includes a Users Manual and an Installation Guide.

1. Long-Slit Spectroscopy

Because of its very low intrinsic background noise and of the absence of readout noise the PCD is particularly well suited to applications where the sky background is low. These situations also allow to exploit the best part of the dynamic range, before saturation sets in. This is certainly the case for the long-slit spectroscopy mode implemented with the Boller & Chivens spectrograph at the ESO/Max-Planck 2.2 m telescope.

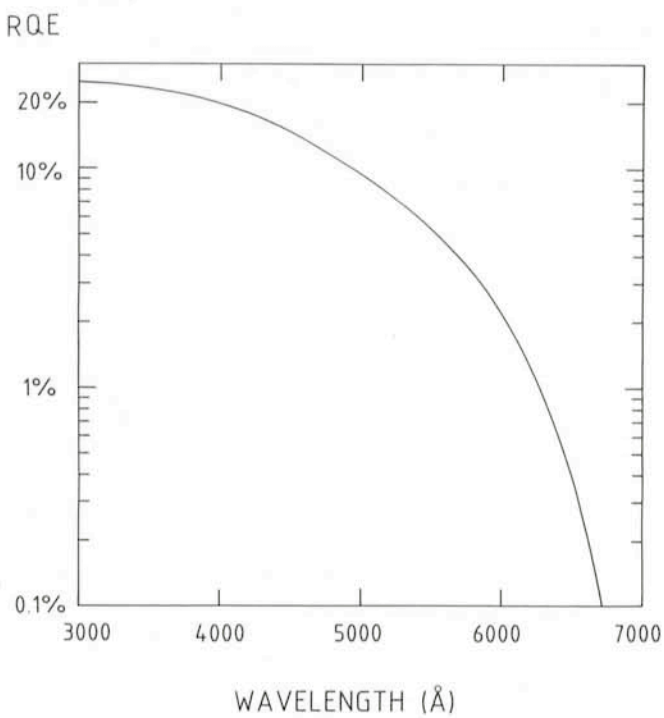

Figure 1: *The responsive quantum efficiency of the PCD image intensifier as measured by the manufacturer.*

* Affiliated to the Astrophysics Division, Space Science Department, European Space Agency.
+ On leave from Osservatorio Astronomico, Padova.

1.1. The New Dioptric Camera

The standard solid Schmidt camera for the B & C spectrograph has too small a back focal distance to be used with the PCD, whose front head is of difficult access because of the permanent magnet surrounding the tube. For this reason a new dioptric camera was designed, tendered out, built and put into operation at the spectrograph. The whole procedure was completed with success in 10 months, that is about one half of the time normally required for this type of project. The optical design was made at ESO and is shown in Figure 2.

Tentative Time-table of Council Sessions and Committee Meetings in 1985

November 12	Scientific Technical Committee
November 13–14	Finance Committee
December 11–12	Observing Programmes Committee
December 16	Committee of Council
December 17	Council

All meetings will take place at ESO in Garching.

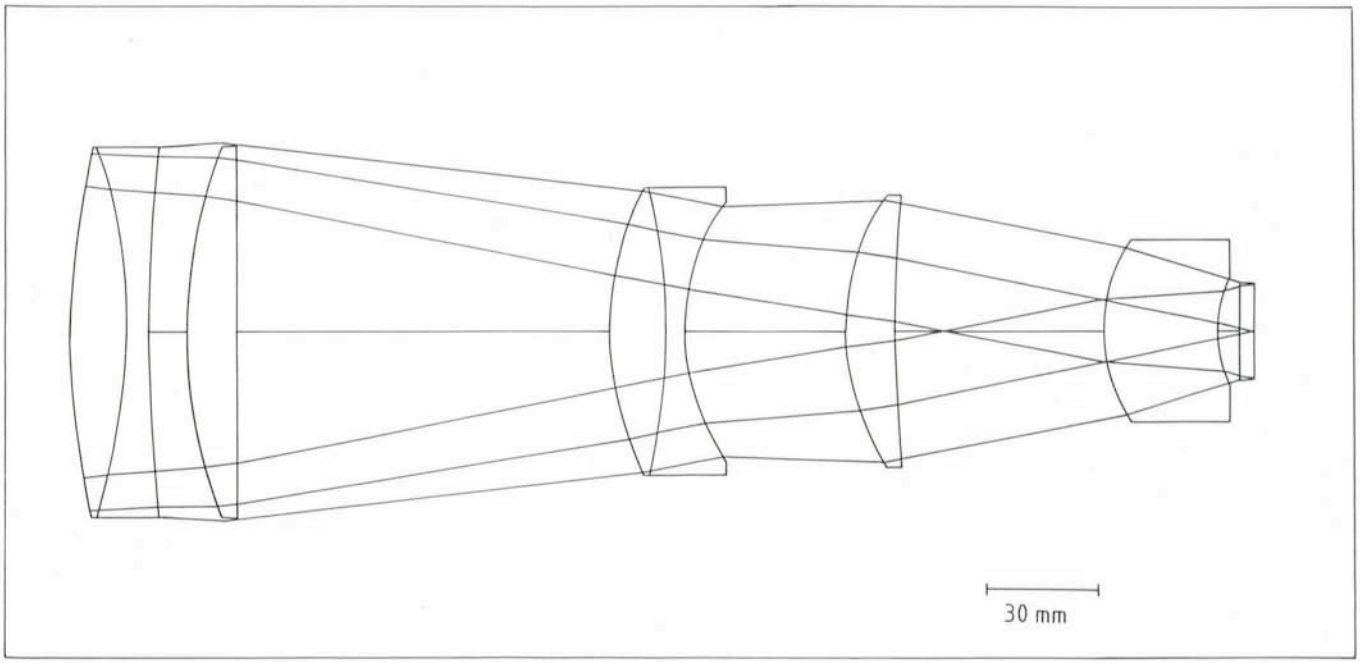

Figure 2: *The optical design of the new dioptric F/2 camera for the Boller & Chivens spectrograph and the ESA PCD.*

The characteristics of the camera are: Focal length : 190 mm; Diameter of the entrance lens : 98 mm; Aperture : F/2; Wavelength range : 3400–6600 Å; Field diameter : 25 mm; Scale factor : 1 arcsec = 22 μm at the detector.

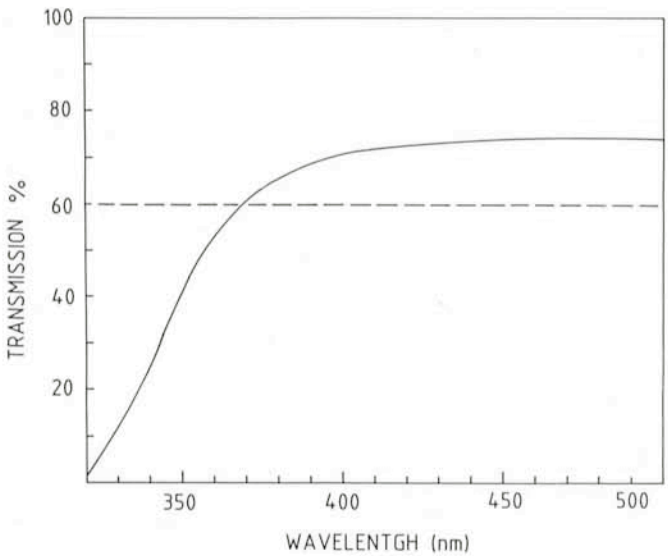

Figure 3: *The transmission of the new F/2 camera as measured at ESO. The broken line shows the average efficiency (transmission and vignetting) of the solid Schmidt camera which is used at the spectrograph with the CCD detectors.*

The image quality is about 20 μm and the vignetting is very small (5% at 10 mm from the axis). The camera was built according to the ESO specifications by the Officine Galileo, Italy. Figure 3 shows the measured transmission curve of the new camera with that computed for the solid Schmidt. The fall at short wavelengths is due to the low UV transmission of the FK 54 glass components of the optical train. By using glass from a melt with a better UV transparency, one should be able to rise the efficiency of the camera at 3500 Å by 15%. This option will probably be implemented at the end of the year.

1.2. Performance

The camera and the detector were mounted at the B & C spectrograph in February 1985 (Fig. 4) and have been used for several observing programs. The standard format used in the spectroscopic mode is 1024 × 256 pixels, 25 μm in size. In a typical configuration, the detector was used with the ESO grating # 7 to work in the blue, UV region. The linear dispersion is then 85 Å/mm, the spectral coverage about 2100 Å. With a slit 1.5 arcsec wide, the average FWHM of the comparison lines is 5 Å. Table 1 shows the characteristics of the gratings recommended for use with the B & C and the PCD.

By observations of standard stars close to the zenith with a widely open slit, we have derived the relative spectral response of the telescope-spectrograph-detector combination when grating # 7 is used (Fig. 5). It is also found that stars of m = 12.6, 13.8 and 13.8 give one count/sec/Å at 3500, 3800 and 4440 Å respectively. In order to stay within the linear part

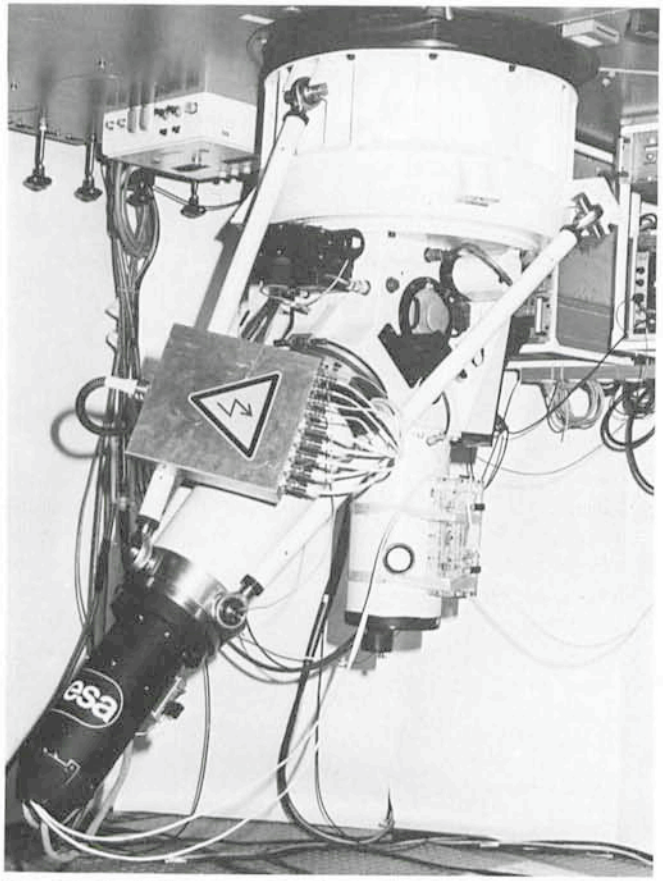

Figure 4: *The PCD mounted on the B & C spectrograph at the 2.2 m telescope.*

of the dynamic range, the observed point sources have to be at least 1.5 magnitudes fainter than those given above, at the same dispersion. Figure 6 shows a spectrum of the radio galaxy PKS 0349−27 after preliminary correction for the image tube distortion.

2. Direct Imaging

To the contrary of the flight version of the FOC, where the very expanded scale and lower sky background of the HST are particularly favorable, the PCD is not suited to broad band imaging, because the sky background considerably reduces the available dynamic range. Nevertheless, a direct imaging mode is implemented at the 2.2 m telescope to be used mainly with narrow-band filters. The PCD with its shutter and filter wheels assembly are mounted on the adapter (Fig. 7), so that the standard TV guider can be used. The standard 512 × 512 pixel format gives a scale of 0.3 and 0.6 arcsec per pixel over a field of 2.5 and 5 arcmin with pixel sizes of 25 and 50 μm respectively. A set of interference filters peaked at the [OII] 3727 Å and [OIII] 5007 Å emission lines is available for various redshifts. An IHAP batch program is normally used to find the best telescope focus from a focus sequence exposure. The same program is used to monitor the image quality, and Figure 8 shows a histogram of the image size (FWHM) over 12 nights

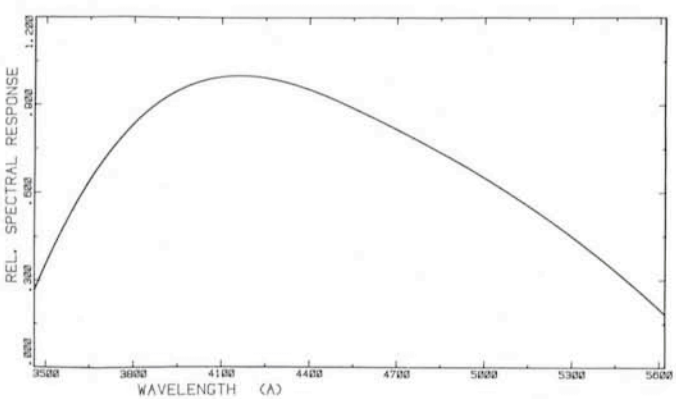

Figure 5: *The spectral response of the telescope-spectrograph-detector combination determined from the observation of a standard star with wide slit. The spectra were taken with the ESO grating # 7, at the blaze angle (8° 38'). The plot is normalized at the peak value.*

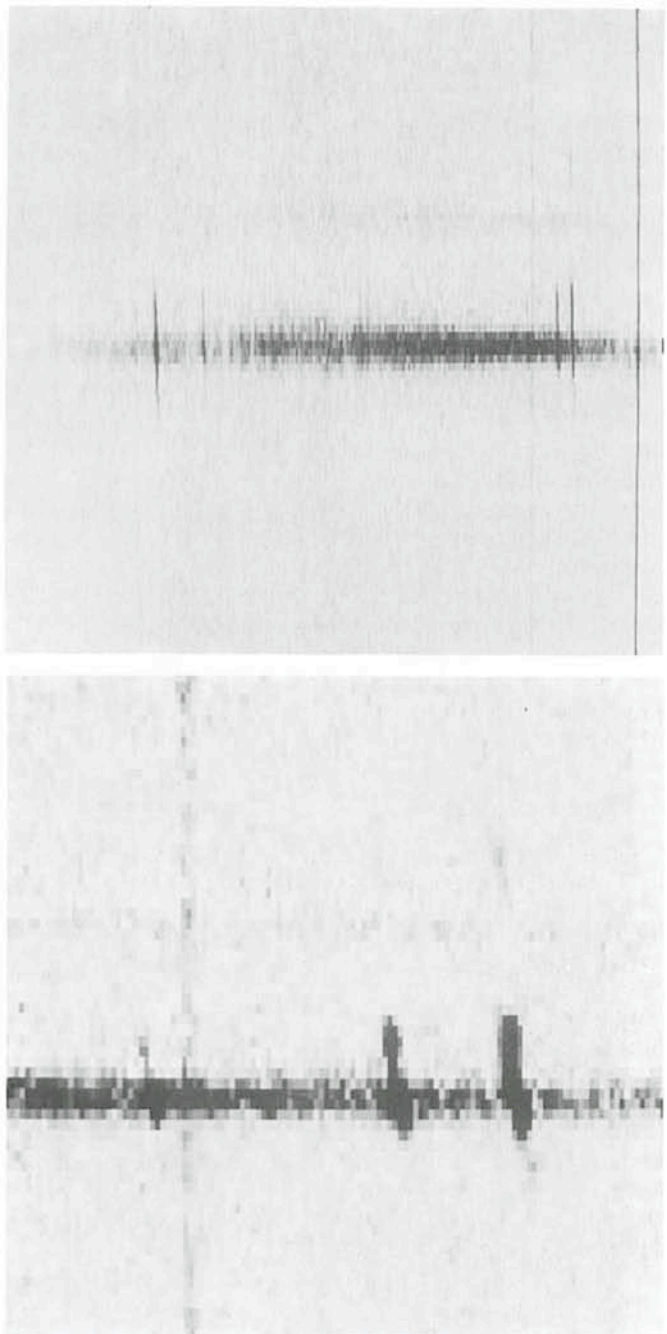

Figure 6: *The PCD spectrum of the radio galaxy PKS 0349−27, taken in a 30-minute exposure with the ESO grating # 7 at blaze angle. The bright nucleus has m (B) = 16.8, while the fainter continuum corresponds to a feature with m (B) = 20. Fig. 6a shows the whole observed range from 3500 to 5600 Å; Fig. 6b is an enlargement of the Hβ and [OIII] region. The geometric distortion has been corrected with IHAP.*

TABLE I

PCD + B & C recommended gratings

ESO grating #	gr/mm	order	Dispersion Å/mm	Dispersion Å/pixel	Peak efficiency	Useful range	Comments
24	400	1	126	3.1	60% at 3000 Å	3000–6200 Å	High UV efficiency
7	600	1	85	2.1	71% at 4400 Å	3500–5600 Å	General purpose
6	600	2	43	1.07	53% at 3500 Å	3200–4200 Å	Medium disp. UV – blue
20	1200	2	21.4	0.53	47% at 4000 Å	500 Å anywhere between 3200 Å and 5300 Å	Highest disp. low eff.
On order	600	1	85	2.1	~70% at 3500 Å	3000–5100 Å	High UV efficiency

last April. We can confirm the careful control of local sources of turbulence at the 2.2 m telescope and we suggest that the high rate of occurrence of 0.7 arcsec image size may be the result of the integration of a "good seeing wing" of a nearly symmetric distribution extending down to 0.3–0.4 arcsec. Very good images would be enlarged to 0.7 arcsec FWHM by effects additional to atmospheric seeing like telescope jitter, local seeing, detector resolution and pixel sampling. More extensive tests are necessary to check this hypothesis and eventually to make better use of the excellent conditions present at La Silla.

3. Data Reduction

At ESO two data reduction systems are available at present. IHAP, based on the Hewlett Packard computers, operates at the telescopes on La Silla and can be used for data reduction in Garching. MIDAS, based on the VAX computer, is intended to become the main data reduction facility for the users of the ESO telescopes and of the HST as far as Europe is concerned. The IHAP system has so far been used for the reduction of PCD data and it has demonstrated to be able to cope with many of the needs. As an example of direct imaging data reduction, Figure 9 shows two images of the radio galaxy PKS 0349–27, in the light of redshifted [OIII] and in the nearby continuum. The third image is the difference of the previous two and shows well the ionized gas present in the galaxy. It was obtained by first geometrically registering the two original images using the positions of the stars in the field, then scaling the results to compensate for the different filter transmission and width, and finally computing a pixel by pixel difference. This procedure has been reasonably satisfactory in detecting very faint extended emission (di Serego Alighieri et al., 1984), although the geometric distortion of the PCD (mostly S distortion in the image tube) cannot be accurately corrected by the translation and rotation commands available in IHAP. Better results can be obtained with the software package developed at Rutherford and Appleton Laboratories for the FOC and now being implemented in MIDAS, which corrects for the geometric distortion using the regular grid of reseaux marks etched on the first photocathode of the PCD. This software can be applied to direct imaging data, when a relatively bright sky background allows the detection of most of the reseaux marks. This is unfortunately not the case for the long-slit spectroscopy mode, where one would also ideally like to correct for the distortions in the spectrograph. In order to make this possible, spectra of the wavelength calibration lamp are taken at the telescope through a decker with a series of

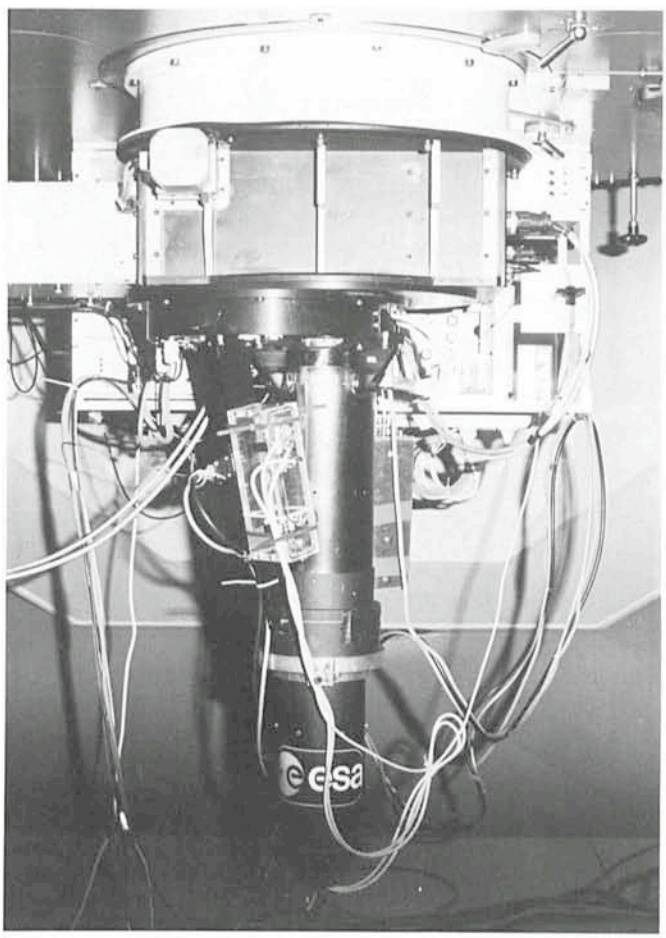

Figure 7: *The PCD mounted on the adapter of the 2.2 m telescope for direct imaging. The square box attached to the telescope flange hosts the TV offset guider, with the PCD filter/shutter unit below.*

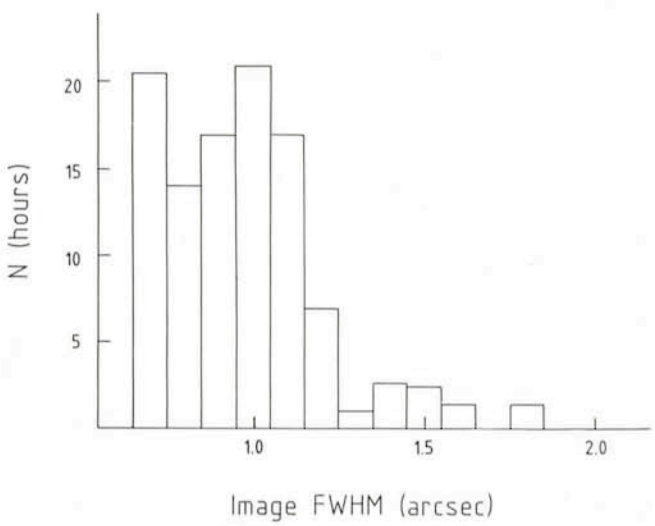

Figure 8: *The histogram of the image size obtained during 12 nights with the PCD in direct imaging mode at the 2.2 m telescope.*

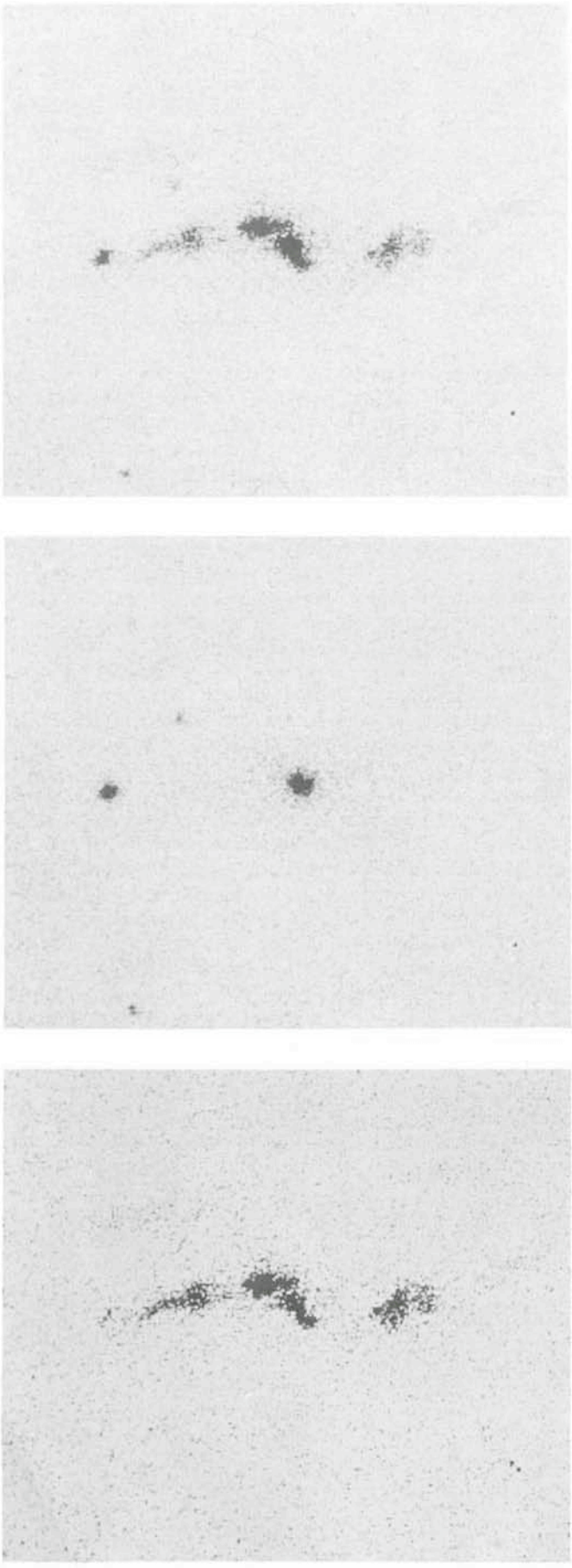

Figure 9: *The field of the radio galaxy PKS 0349–27 in the light of redshifted [OIII] (a), in the nearby continuum (b), and the difference of the previous two (c), showing well the extended ionized gas. North is at the top and east at the left. Picture size is 1.2 arcmin.*

small equispaced holes along the slit (spacing is 25 arcsec, i.e., 22 pixels).

Using these images, the distortion can be preliminarily corrected with a two-step IHAP command sequence operating on a single dimension. The spectrum in Figure 6 has been corrected using this method. A MIDAS procedure is now being developed to operate in the two dimensions in a single step and to transform directly from X, Y pixel coordinates into wavelength and distance along the slit.

4. Acknowledgements

We gratefully acknowledge the skillful help of the ESO technical staff at La Silla, namely Daniel Hofstadt, Paul Le Saux and Eric Allaert, in bringing the PCD into efficient operation. We also like to thank Prof. G. Setti and Dr. B.G. Taylor for their support of the project and for making the rapid conclusion of the ESA/ESO agreement possible.

References

di Serego Alighieri, S., Perryman, M.A.C., Macchetto, F., 1984, *Astrophys. J.* **285,** 567.

di Serego Alighieri, S., Perryman, M.A.C., Macchetto. F., 1985a, *Astron. Astrophys.* **149,** 179.

di Serego Alighieri, S., Perryman, M.A.C., Macchetto, F., 1985b, *ESA Bull.* **42,** 17.

STAFF MOVEMENTS

Arrivals

Europe

KOTZLOWSKI, Heinz (D), Senior Mechanical Engineer
RICHMOND, Alan (GB), Associate
RODRIGUEZ ESPINOSA, José (E), Fellow
WARMELS, Rein (NL), Astronomical Applications Programmer

Chile

MAGAIN, Pierre (B), Fellow

Departures

Europe

BANDIERA, Rino (I), Fellow
BÜCHERL, Helmut (D), Electro-mechanical Technician
GILLET, Denis (F), Fellow
OLIVA, Ernesto (I), Fellow
SADLER, Elaine (GB/AUS), Fellow
SURDEJ, Jean (B), Associate

An ESO/OHP Workshop on

"The Optimization of the Use of CCD Detectors in Astronomy"

will be held at the Observatoire de Haute-Provence from June 17 to 19, 1986.

Topics of discussion will include the performance of the different devices and of the control systems, flat-fielding techniques and data reduction software. Prospects for new developments will also be reviewed. The workshop will be limited to 70 participants. Further information may be obtained from S. D'Odorico at ESO or P. Véron at OHP (F-04870 Saint-Michel l'Observatoire, tel. 0033-92-766368).

Geometric Rectification of PCD and ST-FOC Data with MIDAS

D. Baade[1], D. Ponz[2] and S. di Serego Alighieri[1+]*

[1] *The Space Telescope European Coordinating Facility, European Southern Observatory*
[2] *European Southern Observatory*

It is now about six months since ESA's Photon Counting Detector (PCD), the ground-based counterpart to the Faint-Object Camera (FOC) to be flown with the Hubble Space Telescope, was put into operation at La Silla and made available to Visiting Astronomers. There it proved to be very reliable and, also thanks to good weather conditions, was very productive. By now, quite a few readers of the *Messenger* will be busy analysing their own PCD observations.

The PCD owes its high sensitivity and its ability to count single photon events to a three-stage image intensifier which is the technical heart of the instrument. The price to be paid is the S-like geometrical distortion which is a typical and inevitable property of image tubes. Unlike e.g. the IPCS (Boksenberg 1972) where this distortion is corrected for in one dimension by the hardware so that the correction only needs to be done in the second coordinate, PCD (and FOC) images require a bi-dimensional rectification. To this end, a regular grid of reseaux marks are etched on the first photocathode to provide the necessary reference points. However, they can only be used in the direct imaging mode since only then they stand out dark against the brighter sky background. By contrast, in the long-slit spectroscopic mode the opposite principle has to be adopted where separate calibration images with bright spots are obtained by observing an arc spectrum through a mask with a series of equidistant holes parallel to the spectrograph slit.

So far there was no dedicated software available at ESO to cope with those special requirements of PCD data. On the other hand, the number of totally different steps necessary to reduce any kind of optical astronomical data is not all that large. Owing to the modular structure of MIDAS, it might therefore be possible to merely adapt some existing programs from the growing pool of MIDAS software to this problem.

Let us briefly summarize what one would like to expect from the solution:

(1) find and identify the reseaux marks and comparison spectrum features, respectively,
(2) determine a parametrization of the geometric distortion,
(3) conserve the flux on a small local scale,
(4) handle undersampled data like those of some of the FOC modes,
(5) correct spectral data for geometric distortion and non-linearity of the wavelength scale in one step in order to avoid unnecessary degradation of the data due to multiple rebinning.

The detection and identification of features which combine to a rather similar pattern as in the long-slit spectroscopic mode of the PCD is one of the major steps during the course of the reduction of CASPEC data (cf. MIDAS manual). In fact, in MIDAS this PCD related task can be done on the command procedure level by combining existing CASPEC software modules (Ponz and di Serego Alighieri, in preparation). The MIDAS TABLE system furthermore supports a two-dimensional polynomial regression analysis (so far mostly used for the CASPEC data reduction) required for point 2 on the list above.

Only for the rebinning a new main program had to be written in order to also cope with severely undersampled point spread functions having a FWHM of the order of one detector element (such as in the f/48 mode of the ST-FOC, but also in ground-based PCD data obtained under exceptionally good seeing conditions). Assuming (or in more sophisticated future versions also knowing) the point spread function, the data are first effectively deconvolved and each input pixel subdivided into 3×3 sub-pixels holding the result of the deconvolution. According to the prescriptions found by the two-dimensional regression analysis, the input flux is then dropped sub-pixel by sub-pixel into the grid of again regular-sized pixels defining the geometrically rectified (output) image.

This procedure is faster than to strictly project each sub-pixel onto the output grid because varying (across the image) input-to-output pixel size ratios and orientations do not permit one to define one fixed algorithm to be followed across the entire image. The trade-off is with the local flux conservation whose accuracy obviously deteriorates with increasing size of the sub-pixels. For very high S/N data there is an option to replace each sub-pixel by a number of still smaller units ("substepping", no further interpolation done). Without this additional subdivision an image with uniform flux distribution shows after the rectification little "cracks" with an amplitude of the order of 1 %. Their number is increased but their amplitude is reduced by making use of the sub-stepping option. From the varying input-to-output pixel size ratio it is clear that a small large-scale modulation of the flux density must necessarily be present and that the quality criterion can only be the smoothness of this modulation. The penalty to be paid in terms of CPU time for the usage of a large additional sub-stepping factor is high and only justified in extreme cases.

The most critical test of the usefulness of the polynomial "Ansatz" is obviously provided by the long-slit spectroscopic mode where in the same step not only the geometrical rectification but also the linearization of the wavelength scale is to be accomplished. The results for a test frame with 1024×256 pixels containing a series of 8 vertically offset spectra of a He-Ar lamp in the range 3700 to 5200 Å and with a dispersion of 2.2 Å/pixel are shown in Figures 1a and b. The degree of the polynomial was 3 in both wavelength and position perpendicular to the dispersion direction (the MIDAS regression analysis program used is unusual in that it includes *all* terms $x^m y^n$ with $m \leq$ degree in x, $n \leq$ degree in y). A pairwise cross-correlation analysis between the 8 spectra yielded perfectly symmetric cross-correlation functions with a FWHM only 5 % larger than the auto-correlation function of one spectrum. The inferred off-set in wavelength between the individual spectra was at most 0.35 Å or one-sixth of a pixel. A subsequent secondary analysis of the spectral dispersion in the reduced data confirmed the linearity of the wavelength scale on the same level. Execution time (without additional substepping) for the 2-D regression analysis and the rebinning was close to 20 minutes CPU time on a VAX 780 thus identifying this step of the PCD data reduction as a typical

---

* Affiliated to the Astrophysics Division, Space Science Department, European Space Agency
\+ On leave from Osservatorio Astronomico, Padova

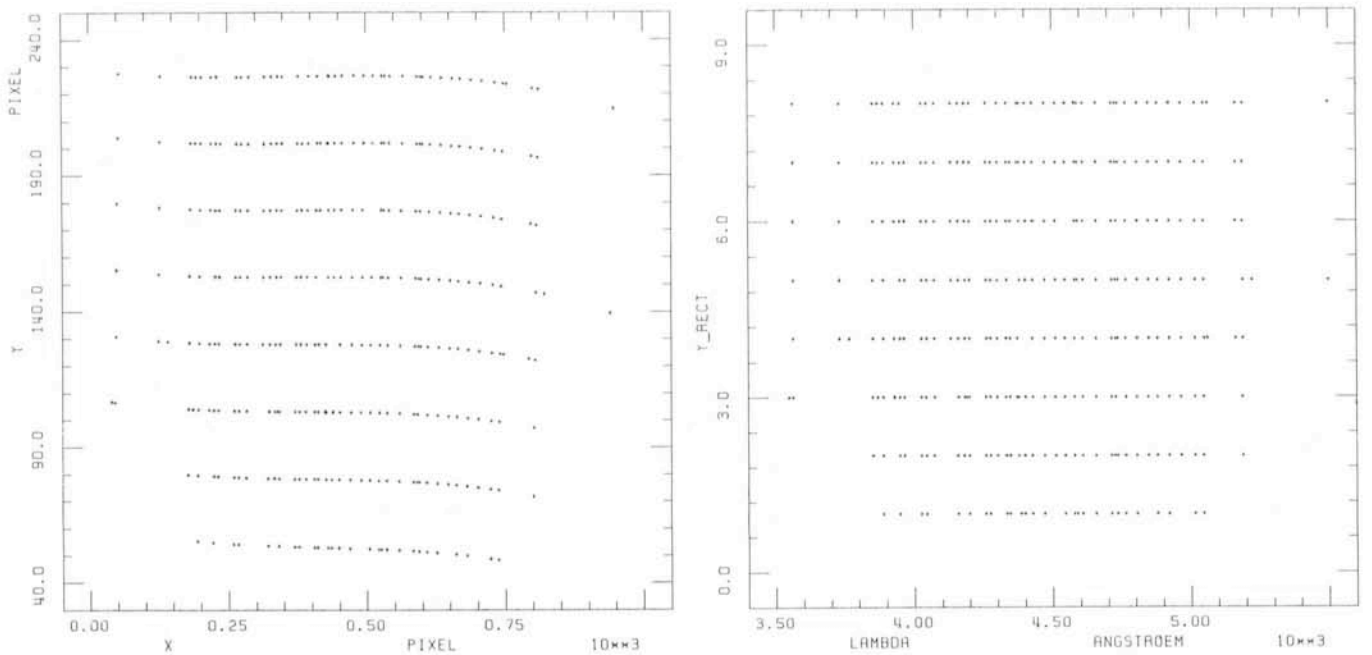

Figures 1 a and b: *The positions of the stronger arc lines (a) in the raw data and (b) after the simultaneous geometrical rectification and rebinning to wavelength. (In Figure 1 a the vertical and horizontal scales are different in order to enhance the visibility of the distortion. The step size in y has been changed from Figure 1 a to b; this is of no relevance.)*

batch task to be executed only at night time. This can be conveniently done, since once reseaux marks and/or comparison spectra are correctly identified, no further user intervention is necessary.

We have written this short note about the reduction of PCD data within MIDAS in order to inform PCD observers about this new possibility to treat their data. We furthermore believe that it is a good example of the growing maturity of MIDAS because more and more problems can now be treated by simply using MIDAS as a high-level problem solving language, often without having to do any FORTRAN coding. After some further improvements have been included, the software described will be available to the MIDAS users community.

References

Boksenberg, A.: 1972, in Proc. ESO/CERN Workshop "Auxiliary Instrumentation for Large Telescopes", eds. S. Laustsen and A. Reiz, Geneva, p. 295.

di Serego Alighieri, S., Perryman, M.A.C., Macchetto, F.: 1985, *Astron. Astrophys.* **149,** 179.

Variations of the High Resolution Hα-line Profiles of the Very Young Stars: HR 5999 and HD 163296

P.S. Thé and H.R.E. Tjin A Djie, Astronomical Institute, Amsterdam
C. Catala, F. Praderie and P. Felenbok, Observatoire de Paris, Meudon

Introduction

It was recognized long ago that the Hα line (6563 Å) is very important for the study of stellar winds in pre-main sequence (PMS) stars (Kuhi 1964). There are two reasons for this. Firstly, the Hα line is usually the most intense emission line in the visible spectrum of PMS stars. It is expected to be formed in an extended region of the wind, thus providing a good global insight tool on the structure of the wind. Secondly, the location of the Hα line in the optical spectrum is such that this line can be very easily observed with Reticon and CCD detectors.

Two southern emission-line stars, HR 5999 and HD 163296, drew much attention lately because these bright A-type objects possess most of the spectacular properties of the so-called Herbig Ae/Be stars (Thé et al. 1985a and Thé et al. 1985b). This class of Herbig (1960) stars was shown by Strom et al. (1972) to consist of younger than main-sequence objects.

In the present short communication the remarkable variations of the Hα profile in HR 5999 during a space/ground-based coordinated campaign in September 1983, and at other epochs, will be discussed. The emission line star HD 163296, originally intended as a comparison star, was also observed at the same observing runs as HR 5999; its Hα profile variation will be shown as well. Suggestions for an interpretation of the Hα-line formation are then presented.

Some Properties of the Hα line in PMS Stars

Finkenzeller and Mundt (1984) have surveyed 57 candidate Herbig Ae/Be stars in the line of Hα, NaI D and HeIλ5876. They conclude that the Herbig Ae/Be stars can be devided in 3 subclasses according to the shape of the Hα-line profile: (1) with a double peak, comprising 50 % of the whole sample; (2) with a single peak (25 %), and (3) with a P Cygni profile (20 %).

A similar survey was reported for T Tauri stars by Kuhi

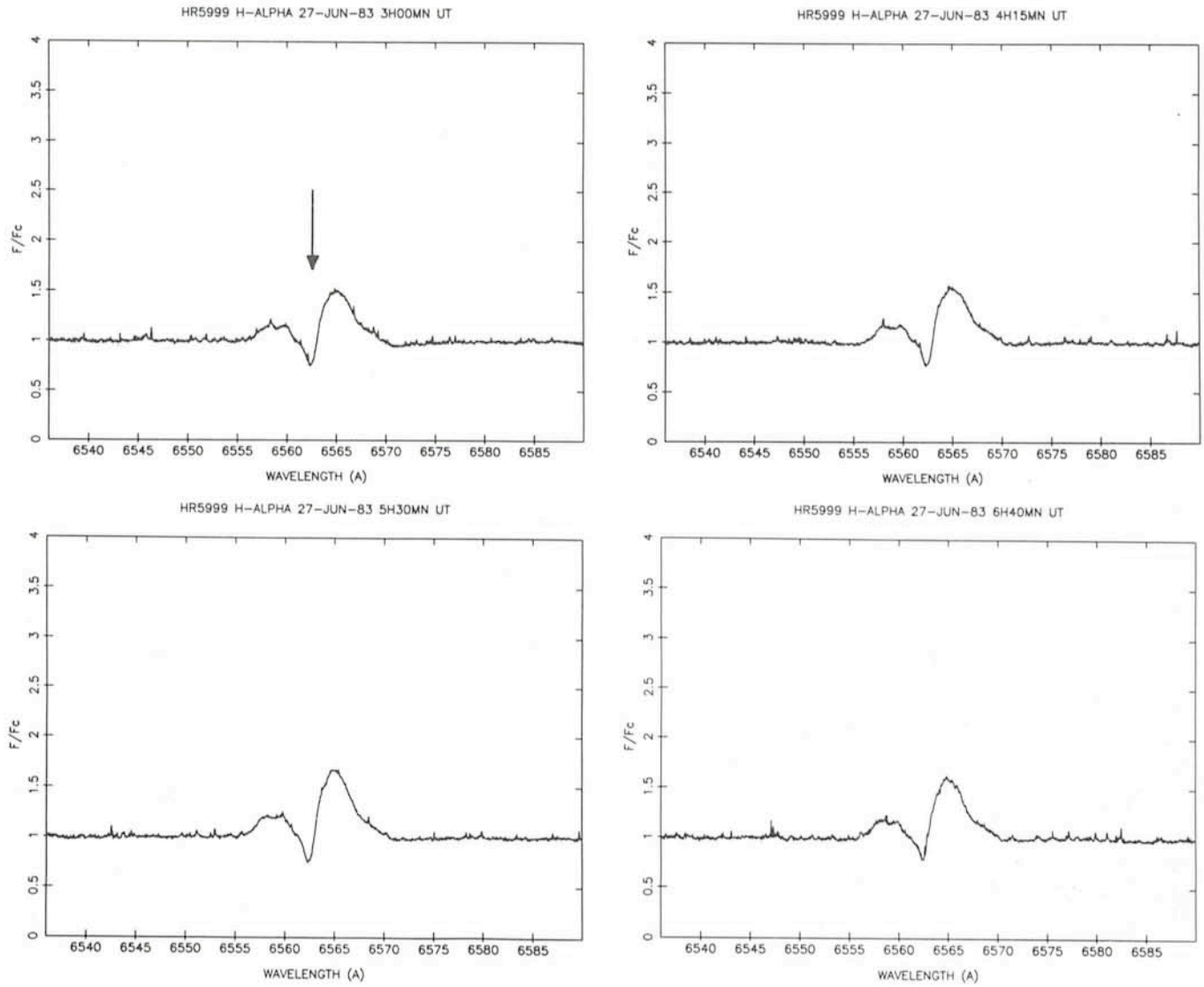

Figure 1: *The Hα line of HR 5999 at four different moments on June 27, 1983. The wavelength scale is in the geocentric frame. The vertical arrow on the first spectrum indicates the absorption trough.*

(1978). Compared to Herbig Ae/Be stars, the T Tauri stars are spectroscopically more difficult to observe in high resolution mode because they are fainter. For this reason 20 % of the 75 stars surveyed by Kuhi (1978) have been inadequately observed for the purpose of an Hα line classification. Among the 75 program stars 60 % have a double peak at Hα, 10 % a single peak, 5 % a P Cygni profile and 5 % a profile with a longward displaced absorption (this could indicate infall of matter). No inverse P Cygni profile has been observed in the Hα line of T Tauri stars.

The basic property that appears from these surveys is that most of the PMS stars show a double peak profile at Hα. However, significant fractions of the observed samples exhibit different kinds of profiles, suggesting that there may exist important differences in the geometry and/or the structure of the extended gaseous envelopes of the two sets of PMS stars. An important question to be addressed is whether these differences correspond to different evolutionary stages.

Observations of HR 5999 and HD 163296

The star HR 5999 (A7 IIIe, V = $6^{m}.8$) was observed with the Coudé Echelle Spectrometer fed by the 1.4 m Coudé Auxiliary Telescope (CAT) at ESO. The detector is a cooled Reticon chip

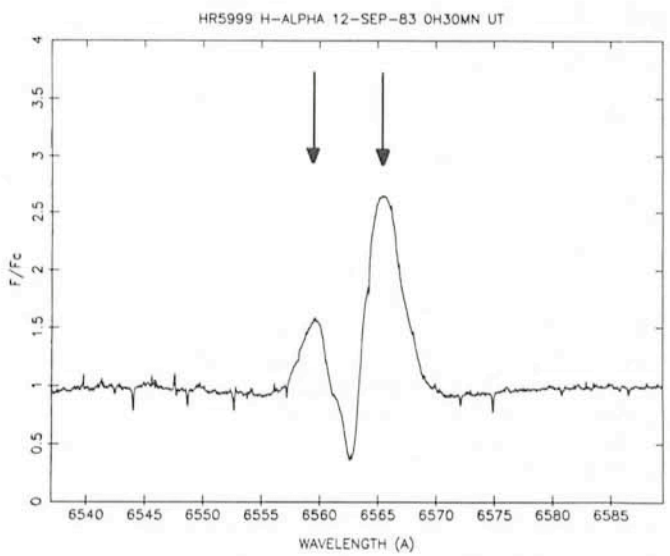

Figure 2: *The same as in Figure 1, but for the September 12, 1983, spectrum. Note that the y-axis scale is the same as in Figure 1. The two vertical arrows indicate the blue and the red emission components.*

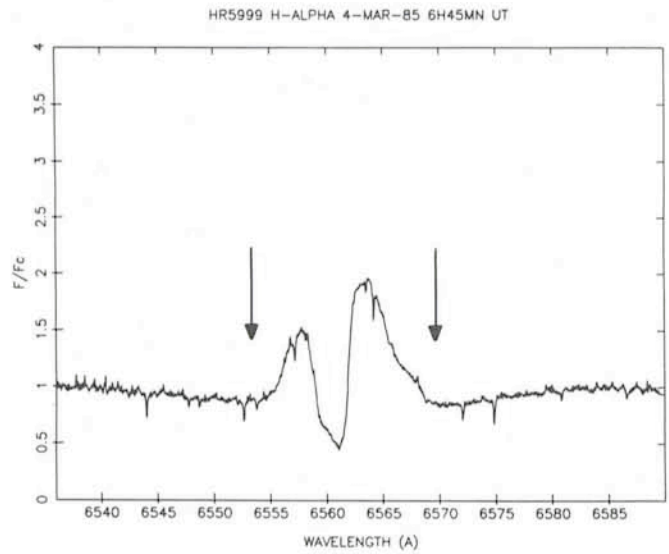

Figure 3: *The same as in Figure 1, but for one of the March 1985 spectra. The two vertical arrows indicate the limits of the emission.*

with 1872 diodes. These high resolution observations were made on June 27, 1983, by P. S. Thé, on September 12, 1983, by R. Faraggiana and on March 3 to 9, 1984, by F. Praderie. They obtained 5, 1 and 10 spectra, respectively, with exposure times of 1 hour or more. An attempt to observe the Hα line simultaneously with the EXOSAT (September 11, 1983, 16–21 hr UT) from the South African Astronomical Observatory (74 inch telescope, image tube spectrograph equipped with a Reticon, resolution 594 mÅ) was totally unsuccessful due to poor weather conditions (F. Praderie, J. W. Menzies).

The spectra obtained at ESO were reduced on the Meudon Observatory VAX computer using the STII interactive software. They are normalized to the continuum. Figure 1 displays four Hα line profiles of HR 5999 observed during one night in June 1983, Figure 2 the profile obtained in September 1983, and Figure 3 one of the spectra observed in March 1985. The hourly variations, the night-to-night as well as the long-term variations (3 and 20 months) of the Hα profile of HR 5999 are not dramatic, although they are more than significant. The global shape of the line remains unchanged, namely a double-peak emission with higher red than blue intensity and an absorption component of which the minimum lies well below the continuum level. This kind of profile is similar to the classical type III P Cygni profile, according to Beals' (1951) classification.

On the June 1983 spectra (Fig. 1) one notes the progressive development of a weak absorption on the blue emission peak of Hα. This feature is absent in September 1983. Furthermore, in September 1983, the two emission components are more intense than in June 1983, and the ratio I_{Red}/I_{Blue} has increased. In March 1985, the absorption trough is much broader and deeper, the emission components are still more intense than in June 1983. The night-to-night variation that we have observed in March 1985 will be described and discussed in a future publication.

It is also remarkable that the wind velocity in the line of sight at large distances from the stellar surface is no more than about 100 km s^{-1}, as indicated by the positional shift of the blue absorption trough in the profile.

The V = $6^{m}.7$ emission line star HD 163296, classified "almost conventional Be" by Allen and Swings (1976), B9 V by Buscombe (1969), A2e by Wilson and Joy (1952), was observed by the same persons using the same instruments and resolution as HR 5999 in June and in September 1983. Figure 4 shows the Hα profiles of HD 163296. The change in profile between the two dates (monthly variations) is impressive. The Hα line shows a type I or II P Cygni profile, with 3 blue absorption components in September 1983, while it was a double-peak emission profile in June; in the blue absorption component(s) the intensity is below the continuum level. The June 1983 profile is somewhat similar to the Hα profile of HR 5999. It should be noted, that a recent (March 1985) IUE observation of the MgII lines of HD 163296 shows the same behavior compared to an old spectrum found in the IUE data bank.

These remarkable long-term variabilities, in particular the fact that a single star can shift from one Hα profile shape to another, argues against the interpretation of the different profile shapes being characteristic of different evolutionary stages. However, HD 163296 does not seem to be a typical Herbig star, because it is not associated with a nebulosity (Thé et al. 1985b), so that no general conclusion about the whole class can be drawn from this result.

It is of interest to understand what kind of atmospheric structure produces these different Hα profiles and their variations.

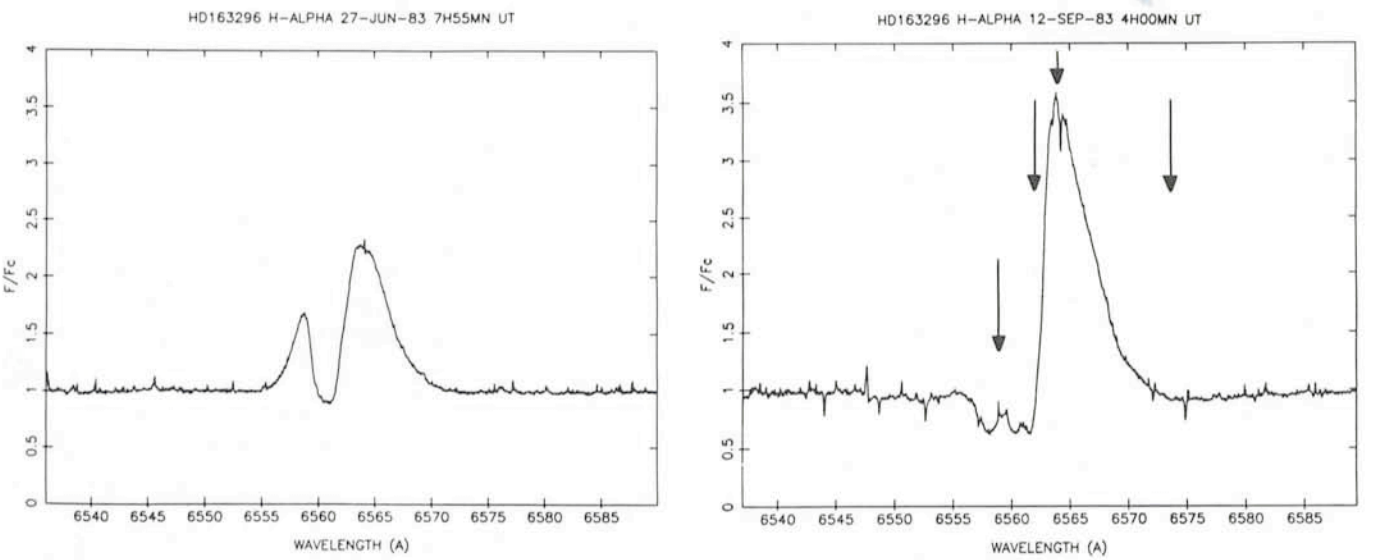

Figure 4: *The Hα line of HD 163296 at two different dates. On the right hand spectrum, the vertical arrows indicate, from left to right: the position of the absorption trough, the blue boundary of the emission component, its position and its red boundary.*

Examples of Qualitative Interpretation

This section deals with the Hα line profile of HR 5999, and with different types of qualitative interpretation for a type III P Cygni profile. We will discuss four examples, which should be considered as incomplete. In particular, these explanations are all based on a spherically symmetric atmosphere. A whole set of different interpretations can probably be found without this assumption.

A first possibility for obtaining a type III P Cygni profile is to assume that the line is formed in a region of the extended atmosphere, which is subject to both differential rotation (rotational velocity decreasing outwards) and an expansion (expansion velocity increasing outwards). This idea was first presented by Mihalas and Conti (1980) to explain such profiles. In this case, a "normal" P Cygni profile is "dug" in the, due to rotation, double-peaked emission profile. A profile like the one shown in Fig. 1 can be formed if the maximum expansion velocity v_{max} is lower than the rotational velocity.

Another possibility that can be considered is that the line is formed in a region containing a chromosphere which is surrounded by a cool decelerating wind. In this case a P Cygni profile is "dug" in the single peak emission profile formed in the chromosphere. It is possible to obtain a profile of the expected shape if outward or inward velocity fields are present in the chromosphere.

The same kind of profile can be produced if a cool expanding envelope surrounds a hot region where high velocity turbulent motions or organized motions (e.g. loops) are present. In this case the maximum expansion velocity of the cool envelope must be lower than the velocity of the motions in the hot region.

As a fourth possibility we suggest that the line is formed in a geometrically thin expanding or infalling shell. It has been shown by Wagenblast, Bertout and Bastian (1983) that a profile of the same shape as the one shown in Figure 1 can be obtained provided certain conditions on the velocity law, the source function and the absorption coefficient are fulfilled.

These four examples show that interpreting a line profile such as the Hα line in HR 5999 is complicated, and that the solution is probably not unique. Since the projected rotational velocity of HR 5999 is fairly high (180 km s^{-1}), since the star is surrounded by a chromosphere and transition region (Tjin A Djie et al. 1982), and since Hα is the major signature of the presence of a stellar wind (but with v_{max} near 100 km s^{-1} it is smaller than the stellar v. sin i), the first three possibilities should certainly be analyzed quantitatively. Note that it is not likely that Hα is optically thin in HR 5999. However, as the star is variable in this line, a spherically symmetric model is certainly not sufficient.

Concluding Remarks

The Hα-line profile varies in HR 5999 on three characteristic time scales: hourly, nightly and monthly. In HD 163296 only the last two time scales have been observed so far. Both stars are A-type presumably very young objects. As in T Tauri stars, the cause of the spectroscopic variations is still unknown. Whether it is intrinsic to the stars (activity phenomena) or extrinsic (phenomena affecting the circumstellar envelope) is still to be investigated.

References

Allen, D.A. Swings, J.-P.: 1976, *Astron. Astrophys.* **47,** 393.
Beals, C.: 1950, *Publ. Dom. Astrophys. Obs.* **9,** 1.
Buscombe, W.: 1969, *Mon. Not. R. Astr. Soc.* **144,** 31.
Finkenzeller, V., Mundt, R.: 1984, *Astron. Astrophys. Suppl.* **55,** 109.
Herbig, G.H.: 1960, *Astroph. J. Suppl.* **6,** 337.
Kuhi, L.V., 1964, *Astroph. J.* **140,** 1409.
Kuhi, L.V., 1978, in *Protostars and Planets,* ed. T. Gehrels, Tucson, Univ. of Arizona Press, p. 708.
Mihalas, D., Conti, P.S., 1980, *Astroph. J.* **235,** 515.
Strom, S.E., Strom, K.M., Yost, J., Carrasco, L., Grasdalan, G.: 1972, *Astroph. J.* **173,** 353.
Thé, P.S., Tjin A Djie, H.R.E., Brown, A., Catala, C., Doazan, V., Linsky, J.L., Mewe, R., Praderie, F., Talavera, A., Zwaan, C.: 1985a, *Irish Astronomical Journal,* in press.
Thé, P.S., Felenbok, P., Cuypers, H., Tjin A Djie, H.R.E.: 1985b, *Astron. Astrophys.,* in press.
Tjin A Djie, H.R.E., Thé, P.S., Hack, M., Selvelli, P.L.: 1982, *Astron. Astrophys.* **106,** 98.
Wagenblast, R., Bertout, C., Bastian, V.: 1983, *Astron. Astrophys.* **120,** 6.
Wilson, R.E., Joy, A.H.: 1952, *Astroph. J.* **115,** 157.

The Photometric Capabilities of the IDS System

E.J. Wampler, ESO

In the early days of the IDS development crude tests of the system indicated that its response was approximately linear with intensity (McNall, Robinson and Wampler, *Pub. A.S.P.* **82,** 488, 1970; C.M. Gaskell; J.A. Baldwin, private communication). In the March 1985 issue of the *Messenger* (No. 39, p.15) M. Rosa pointed out that the response of the IDS system depended on the intensity of the input light source. The correction formula that he gives in his article is equivalent to stating that the output signal of the IDS has the following dependence on the input light intensity:

$$[\text{Signal}] = [\text{intensity}]^{1.04 \pm 0.02}. \quad (1)$$

This result was obtained by comparing the observed to the theoretical intensities of the [OIII] λλ 4959,5007 doublet and the relative intensities of lines in the Balmer series.

In March 1984 Kris Davidson reached an identical conclusion. In a letter to R.J. Dufour (private communication) he described his study of the intensity ratio of the [OIII] λλ 4959,5007 doublet together with laboratory experiments using neutral density filters, and emission line lamps together with continuum lamps. The result of this study was that the intensity was related to the signal by an identical formula to that given above. The only difference was that Davidson gave ±0.01 as the error of measurement.

Finally, as part of a program to determine the luminosities of bright quasars, Wampler and Ponz (*Ap.J.* **298,** XXX, 1985) compared IDS magnitudes with those obtained by O. Eggen (*Ap.J. Suppl.* **16,** 97, 1968). They found that over a 5 magnitude range in intensities a 0.2 magnitude correction to the IDS data was needed in order to get agreement with the Eggen photomultiplier data. This 0.2 magnitude correction is exactly what would be needed if the relationship between signal and intensity were given by formula 1. Thus the reality of the nonlinearity seems to be very well established and the value of the

power law exponent seems to be well determined.

This non-linear response explains why the IDS sometimes gives poor sky cancellation even when very high signal-to-noise ratios are achieved. If ϱ is the ratio of the input photon rate from the sky to the rate from the star and if R is the ratio of the observed star signal to the signal that would have been observed in the absence of a sky background then clearly

$$R = (1+\varrho)^{1.04} - \varrho^{1.04}. \quad (2)$$

This reduces to

$$R \approx 1.04\,\varrho^{0.04} \quad (3)$$

if $\varrho \gg 1$, and similarly, if $\varrho \ll 1$ then,

$$R \approx 1 + \varrho\,[1.04 - \varrho^{0.04}]. \quad (4)$$

Strong night sky emission lines will leave a positive residual that can be quite large unless the star signal is also very strong. In addition, emission line intensities in the star signal will be slightly overestimated if there is a strong sky or star continuum background.

Besides the non-linearity in the system response as a function of intensity there is a non-linearity to the system response as a function of time. The output signal of the IDS increases with increasing exposure time. This was first noted by P.M. Rybski (*Bull. A.A.S.* **12,** 751, 1980). According to Rybski the phenomenon is repeatable and intensity independent. Thus it is possible to avoid the most serious errors by adopting proper observing procedures. Wills, Netzer, and Wills (*Ap. J.* **288,** 94, 1985) describe one such technique in the appendix to their paper on broad emission features in quasars. It is clear that if the integration periods used on the program objects are significantly greater than the integration periods used for standard stars, the program stars may appear systematically brighter than they actually are by a few tenths of a magnitude. In any case very short exposure times on the standard stars should be avoided.

The causes of these non-linearities are unknown to me. As Rybski (*Bull. A.A.S.* **12,** 751, 1980) has pointed out, a model with an exponential decay and a power law increase approximately fits his data. Deviations from this simple model might account for the effect seen in the non-linearity of response of the detector to different input light intensities. One could speculate that metastable states in the phosphor screen increase the efficiency of the phosphor as the input photoelectron flux increases. Clearly all detector systems that work by measuring the intensity of the phosphor screens of image tubes might be expected to show similar response characteristics.

The effects listed above are important at the 5 %–20 % level but they can be corrected to the 1 % level. With care, and with proper attention to the standard star calibration it should be possible to obtain absolute spectrophotometry accurate to a few percent with the IDS system.

I would like to thank Peter Shaver and Michael Rosa for their suggestions and help in improving this note.

Rotational Velocity of F-type Stars

G. Noci[1], S. Ortolani[2] and A. Pomilia[1]

[1] *Istituto di Astronomia, Università di Firenze*
[2] *Osservatorio Astronomico di Asiago*

The rotation is a general property of celestial objects, which is probably generated by the vorticity of the interstellar matter. Obviously, stars forming from turbulent vortices conserve some of the initial angular momentum, depending on the early formation history. It is well known that there is a well-determined trend of the rotational velocity of main sequence and giant stars with the spectral type. This is shown by the continuous and dashed curves of Figure 1, which are from the paper of Bernacca and Perinotto (*A.A.*, **33,** 443, 1974). Early-type stars have high rotational velocities, while late-type stars are slow rotators. There is a sharp drop in the velocities from F0 to F5, particularly for main sequence stars: stars later than F5 have all very little angular momentum. This has been attributed to the presence of planets around late-type stars, which would contain most of the angular momentum of the system, as it happens in the case of the solar system. The angular momentum is probably transferred during the T Tauri pre-main-sequence phase. Another possibility suggested for the rotation velocity drop is the loss of angular momentum caused by stellar winds, which should occur for stars having convective layers close to the surface, i.e. late-type stars.

Hence the study of the stellar rotation is of great importance in astrophysics and, in particular, in the study of planetary formation. Recent studies show that fast and slow rotators differ also in other properties. It appears (Pallavicini et al., *Ap. J.*, **248,** 279, 1981) that G to M type stars have the rotational velocity proportional to the X-ray luminosity, while for early-type stars there is no such correlation, but rather a correlation between X-ray luminosity and bolometric luminosity.

In the case of late-type stars, the superficial magnetic fields, which are thought to be the cause of the X-ray emission in these stars, are due to a dynamo process which depends on the rotational velocity. F-type stars are important because at this type there must be the transition to a different mechanism

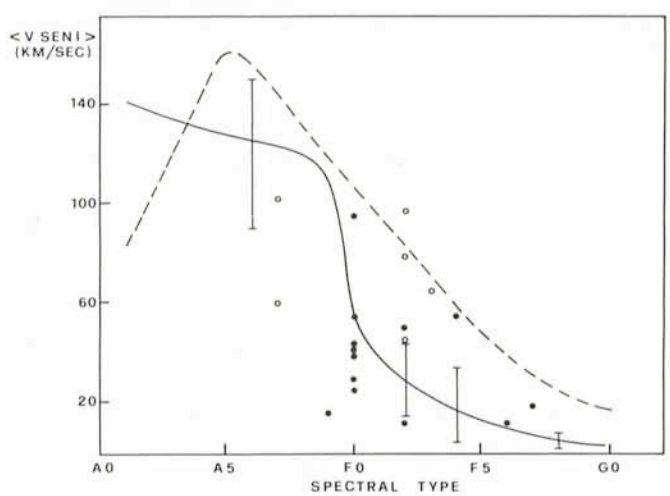

Figure 1: *Rotational velocity vs. spectral type. The continuous and dashed curves (for main sequence and giant stars) are taken from Bernacca and Perinotto (1974). Open circles: giant stars. Filled points: main sequence stars.*

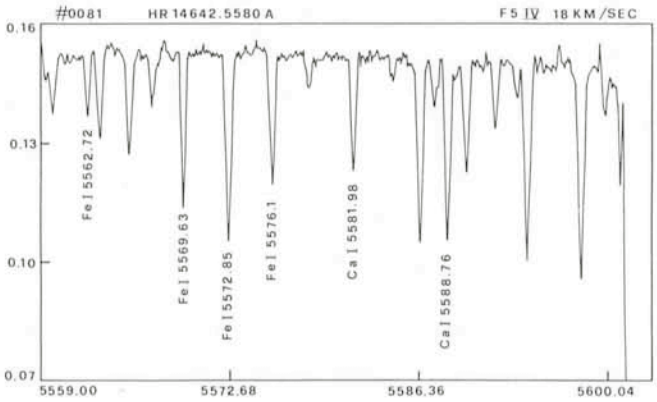

Figure 2: *CES spectrum of the star HR 14642. Some of the most prominent absorption lines are indicated. The star has a rotational velocity v seni = 18 km/sec.*

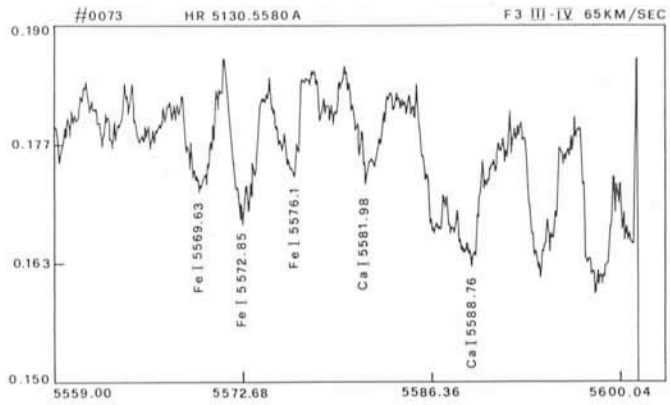

Figure 3: *CES spectrum of the fast rotating star HR 5130 (v seni = 65 km/sec). The wavelength scale is the same as in Fig. 2.*

of X-ray production. The number of F-type stars analyzed so far for rotational velocity is not large. To increase this number we observed a sample of 15 bright, X-ray emission stars at La Silla with the 1.4 m CAT telescope equipped with the CES.

Observations with the CAT

The rotational velocity of a star can be measured, following the classical procedure, from its broadening effect on the photospheric absorption lines, caused by the Doppler effect.

A simple cross correlation between the spectrum of the star to be measured and that of a template star was used to measure the observable quantity, namely v seni (v is the equatorial rotation velocity, i the angle between the rotation

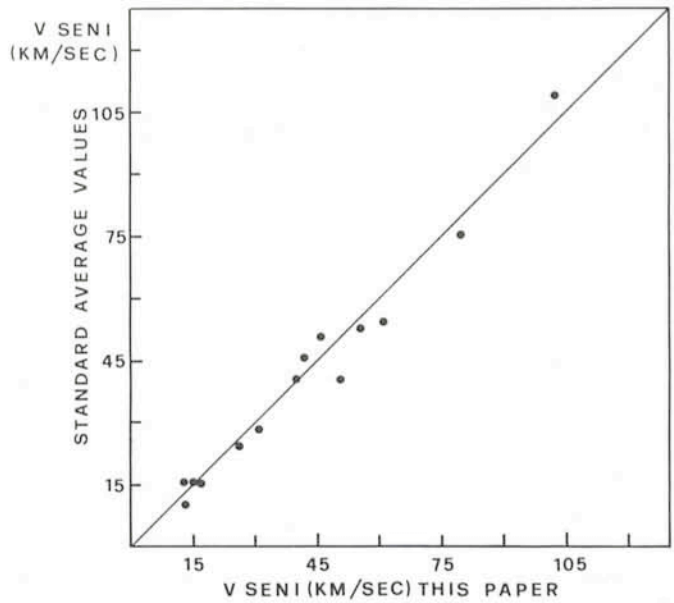

Figure 4: *Rotational velocities calculated with the cross correlation method plotted versus weighted averages from other authors.*

axis and the line of sight). The quality of the spectra is very high, with a resolution of about 80,000, as measured from a laser line. Figures 2 and 3 show two of the spectra obtained during the observations carried out in December 1983 and April 1984. The lines are well defined and the rotational broadening appears evident comparing the two spectra; the spectral region selected is the result of a compromise between the spectral sensitivity of the detector/spectrograph and the need to have several unblended lines of intermediate intensity.

To check our results we have observed, beyond the sample quoted above, 14 stars of known rotational velocity. The velocities obtained by us are plotted in Figure 4 versus the velocities obtained by other authors (weighted averages): the high accuracy of our results and the absence of a systematic deviation are remarkable.

Given the fact that our results appear to be among the best available so far, we are confident that the knowledge of the X-luminosity/v seni relation will be improved. However, we have not yet all the available X-ray data. A comparison of the obtained v seni values with the spectral type confirms the results of previous observations (Fig. 1), both for main-sequence and giant stars. (It must be taken into account that seni can be very small for some stars.) A more extended project, which concerns a wider range of spectral types and includes also echelle spectra obtained at the Asiago Astrophysical Observatory, is under development.

Visiting Astronomers (October 1, 1985 – April 1, 1986)

Observing time has now been allocated for period 36 (October 1, 1985 – April 1, 1986). The demand for telescope time was again much greater than the time actually available.

The following list gives the names of the visiting astronomers, by telescope and in chronological order. The complete list, with dates, equipment and program titles, is available from ESO-Garching.

3.6 m Telescope

Oct. 1985: Kudritzki/Gehren/Husfeld/Hummer/Conti/Méndez/Niemela, Spite, M./Spite, F., Hunger/Heber, Brinks/D'Odorico/Ponz, Bergeron/D'Odorico, Alloin/Pelat, Caputo/Castellani/Saraceno/De Stefanis, Brahic/Sicardy/Roques, Danks/Le Bertre/Chalabaev/Bouchet, Danziger/Oliva/Moorwood, Moorwood/Oliva, Encrenaz/Lecacheux/Combes, Leinert/Dyck.

Nov. 1985: Leinert/Dyck, Marano/Zitelli/Zamorani, Röser/Meisenheimer, Butcher/Mighell/Oemler, Danziger/Rosa/Matteucci, Danziger/Gilmozzi/Kunth, Pizzichini/Pedersen, D'Odorico/Azzopardi/Lequeux/Prévot M. L., Rodono/Foing/Cutispoto/Scaltriti/Bonnet/Linsky/Butler/Haisch.

Dec. 1985: Swings/Gosset/Surdej, de Souza/Quintana, Lequeux/Azzopardi/Breysacher/Muratorio/Westerlund, Azzopardi/Gathier/Meysonnier, Schnur/Arp, Pakull/Angebault/Bianchi/Ilovaisky/Beuermann, Westerlund/Azzopardi/Breysacher/Rebeirot, Jörsäter/Lindblad/Athanassoula, Westerlund/Azzopardi/Breysacher/Rebeirot, Schnur/Schmidt-Kaler/Feitzinger, Balkowski/Boisson/Durret/Rocca Volmerange, Danks/Le Bertre/Chalabaev/Bouchet, Moneti/Natta/Stanga.

Jan. 1986: Moneti/Natta/Stanga, Bergeron/D'Odorico, Koester/Weidemann, Chmielewski/Jousson, Kudritzki/Simon/Méndez.

Feb. 1986: Pottasch/Mampaso/Manchado, Rosino/Ortolani, Ortolani/Gratton, Shaver/Cristiani, Heckman/Miley, Pickles/van der Kruit, D'Odorico/Clowes/Keable.

March 1986: Appenzeller/Östreicher, Dennefeld, Festou/Dennefeld, Véron, Danziger/Binette/Matteucci, Pottasch/Dennefeld/Karoji/Belfort, Courvoisier, Perrier/Encrenaz/Chelli/Colom, de Muizon/d'Hendecourt/Perrier, Preite-Martinez/Persi/Ferrari-Toniolo/Pottasch, Encrenaz/Lecacheux/Combes, Danks/Le Bertre/Chalabaev/Bouchet, Courvoisier, Pottasch/Bouchet/Karoji/Dennefeld/Belfort.

1.4 m CAT

Oct. 1985: Barbieri/Benacchio/Nota, Crivellari/Blackwell/Beckman/Arribas, Crivellari/Beckman/Foing, Heske/Wendker, Holweger/Steenbock, Foing/Bonnet/Crivellari/Beckman/Galleguillos/Lemaire/Gouttebroze.

Nov. 1985: Querci M./Querci F./Yerle/Bouchet, Foing/Bonnet/Crivellari/Beckman/Galleguillos/Lemaire/Gouttebroze.

Dec. 1985: Lindgren/Ardeberg/Maurice, Pallavicini/Pasquini, Waelkens, Pallavicini/Pasquini, Waelkens, Didelon, Waelkens, Gratton/Sneden, Waelkens, Gratton/Sneden.

Jan. 1986: Gratton/Sneden, Barbuy, Vidal-Madjar/Ferlet/de Grijp/Paresce, Ferlet/Vidal-Madjar/Lagrange, Ferlet/Vidal-Madjar/Gry/Laurent/Lallement, Lucy/Baade, Baade/Gathier, Barbieri/Benacchio/Cristiani/Nota, Gillet.

Feb. 1986: Gillet, Lindgren/Ardeberg/Maurice, Gustafsson/Andersen/Edvardsson/Nissen.

March 1986: Cayrel de Strobel, Stalio/Porri, Ruiz/Melnick/Ortiz, Arpigny/Dossin/Manfroid, Danks/Chalabaev/Zuiderwijk/Lambert.

2.2 m Telescope

Oct. 1985: Danziger/Focardi, Jakobsen/Perryman/Blades, Courvoisier/Fosbury/Harris/Gry, Colina/Perryman/Kollatschny, Rafanelli/Schulz/di Serego Alighieri, Chiosi/Bertelli/Ortolani/Gratton, Danziger/Fosbury/Tadhunter.

Dec. 1985: Butcher/Gathier/Buonanno/Mighell, Fusi Pecci/Buonanno/Corsi/Renzini, Pizzichini/Pedersen, Cristiani/Nota, Jörsäter/Lindblad/Athanassoula, Franx/Illingworth.

Jan. 1986: Bottema/van der Kruit, Monnet/Bacon/Martinet, Gathier/Kwitter, Paresce/Vidal-Madjar/de Grijp, Perryman/van Heerde, van Heerde/de Grijp/Lub, Weigelt/Baier/Koller/Kollatschny/Nota.

Feb. 1986: Weigelt/Baier/Koller/Kollatschny/Nota, Jörgenssen/Hansen/Norgaard-Nielsen/de Jong, Reipurth, Weigelt/Baier/Koller/Kollatschny/Nota.

March 1986: Pottasch/Dennefeld/Karoji/Belfort, Brand/Wouterloot.

1.5 m Spectrographic Telescope

Oct. 1985: Seggewiss/Nelles, Alloin/Pelat, Bues/Rupprecht/Pragal, Gry/Vauclair, Gomez/Gerbaldi/Floquet/Grenier.

Nov. 1985: Gomez/Gerbaldi/Floquet/Grenier, v. Amerongen/v. Paradijs/Pakull/Pietsch, Fricke/Hellwig, Alloin/Pelat, Hahn/Lagerkvist/Rickman, Crivellari/Beckman/Foing, Schober/Albrecht, Labhardt.

Dec. 1985: Labhardt, Schoembs/Haefner/Barwig/Mantel/Marschhäuser, Heydari-Malayeri/Testor, Ruiz/Rubio/Pena, Lub/de Ruiter, Schoembs/Haefner/Barwig/Mantel/Marschhäuser, Thé/Westerlund/Pérez.

Jan. 1986: Thé/Westerlund/Pérez, Richtler/Seggewiss, Maciel/Barbuy/Aldrovandi/Faundez-Abans, Lindgren/Ardeberg/Maurice/Prévot L., Rampazzo, Acker/Stenholm/Lundström, Bässgen/Grewig/Krämer/Maluck, Vernin/Azouit.

Feb. 1986: Vernin/Azouit, Strupat/Drechsel/Haug/Böhnhhardt/Rädlein/Rahe, Vernin/Azoit, Thé, Jorissen/Arnould.

March 1986: Jorissen/Arnould, Lagerkvist/Rickman/Hahn/Magnusson, Schneider/Maitzen/Catalano F., Metz/Haefner/Roth, Arpigny/Dossin/Manfroid, Stanga/Falciani/Moneti/Tozzi, Arpigny/Dossin/Manfroid, de Vries J.S.

1 m Photometric Telescope

Oct. 1985: Clementini/Cacciari/Prévot L./Lindgren, Bues/Rupprecht/Pragal, Liller/Alcaino, Bues/Rupprecht/Pragal, Heske/Wendker, Oliva.

Nov. 1985: Oliva, Encrenaz/Lecacheux/Combes, Beuermann/Pakull/Schwope/Pietsch, Motch/Mouchet/Bonnet-Bidaud/Watts, Arlot/Thuillot/Morando/Lecacheux, Motch/Mouchet/Bonnet-Bidaud/Watts, Rodono/Foing/Cutispoto/Scaltriti/Bonnet/Linsky/Butler/Haisch, Hahn/Lagerkvist/Rickman, Crivellari/Beckman/Foing.

Dec. 1985: Crivellari/Beckman/Foing, Danks/Le Bertre/Chalabaev/Bouchet, Trefzger/Labhardt/Spaenhauer/Steinlin, Schoembs/Haefner/Barwig/Mantel/Marschhäuser, Thé/Westerlund/Pérez, Danks/Le Bertre/Chalabaev/Bouchet.

Jan. 1986: Bouvier/Bertout, Richtler, Mermilliod/Claria, Vogt.

Feb. 1986: Vogt, Barwig/Dreier/Haefner/Mantel/Schoembs, Reipurth, Thé, Lagerkvist/Rickman/Hahn/Magnusson.

March 1986: Lagerkvist/Rickman/Hahn/Magnusson, Schneider/Maitzen/Catalano F., Jockers/Geyer/Hänel/Nelles, Hänel/Geyer/Jockers, Pakull/Beuermann/Weißsieker/Reinsch, Stanga/Natta/Moneti/Lenzuni, Stanga/Falciani/Moneti/Tozzi, Danks/Le Bertre/Chalabaev/Bouchet, Persi/Preite-Martinez/Ferrari-Toniolo.

50 cm ESO Photometric Telescope

Oct. 1985: Grenon/Grewing/Scales, Gustafsson/Morell/Edvardsson, Grenon/Grewing/Scales, Arlot/Thuillot/Morando/Lecacheux, Grenon/Grewing/Scales, Arlot/Thuillot/Morando/Lecacheux, Grenon/Grewing/Scales, Gutekunst/Grewing/Bässgen/Kappelmann/Bianchi, Arlot/Thuillot/Morando/Lecacheux, Gutekunst/Grewing/Bässgen/Kappelmann/Bianchi.

Nov. 1985: Gutekunst/Grewing/Bässgen/Kappelmann/Bianchi, Arlot/Thuillot/Morando/Lecacheux, Hahn/Lagerkvist/Rickman, Rodono/Foing/Cutispoto/Scaltriti/Bonnet/Linsky/Butler/Haisch, Arlot/Thuillot/Morando/Lecacheux, Rodono/Foing/Cutispoto/Scaltriti/Bonnet/Linsky/Butler/Haisch, Hahn/Lagerkvist/Rickman.

Dec. 1985: Hahn/Lagerkvist/Rickman, Pedersen/Angebault/Cristiani/Danziger/Gouiffes/Hurley/Lund/Motch/Pietsch/Pizzichini/Poulsen/Rieger.

Jan. 1986: Pedersen/Angebault/Cristiani/Danziger/Gouiffes/Hurley/Lund/Motch/Pietsch/Pizzichini/Poulsen/Rieger, Roddier C./Roddier F.

Feb. 1986: Roddier C./Roddier F., Thé, Schneider/Maitzen.

March 1986: Schneider/Maitzen, Kohoutek/Schramm/Kleine, Metz/Haefner/Roth, Carrasco/Loyola, Manfroid/Sterken/Arpigny.

GPO 40 cm Astrograph

Oct. 1985: Richter/Russell, Tucholke.

Feb. 1986: Debehogne/Machado/Caldeira/Vieira/Netto/Zappala/De Sanctis/Lagerkvist/Mourao/Tavares/Nunes/Protitch-Benishek/Bezerra, Richter/Russell.

March 1986: Ferreri/Zappala/Di Martino/De Sanctis.

1.5 m Danish Telescope

Oct. 1985: Clementini/Cacciari/Prévot L./Lindgren, de Vries C.P./Le Poole, Martinet/Bacon, Brinks/Klein/Dettmar/Danziger/Matteucci, Bosma/Athanassoula, Boisson/Ward, Thomsen et al.

Nov. 1985: Thomsen et al., Walker/Andersen/Storm.

Dec. 1985: v. Paradijs/v.d. Klis, Pedersen, de Souza/Quintana, Pakull/Angebault/Bianchi/Ilovaisky/Beuermann, Heydari-Malayeri/Testor, Bonnet-Bidaud/Gry, de Grijp/Lub/Miley, Hansen.

Jan. 1986: Hansen, Reiz/Piirola, Lindgren/Ardeberg/Maurice/Prévot L., Andersen/Nordström/Olsen.

Feb. 1986: Andersen/Nordström/Olsen, Mayor/Duquennoy/Andersen/Nordström, Mayor/Mermilliod, Hermsen/Pedersen/Spoelstra, Lindgren/Ardeberg/Maurice/Prévot L., Andersen/Nordström, Thomsen et al.

March 1986: Thomsen et al., Reipurth, Andersen/Nordström.

50 cm Danish Telescope

Oct. 1985: v. Paradijs/Henrichs/Trachet, Foing/Bonnet/Crivellari/Beckman/Galleguillos/Lemaire/Gouttebroze.

Nov. 1985: Foing/Bonnet/Crivellari/Beckman/Galleguillos/Lemaire/Gouttebroze, Group for Long Term Photometry of Variables.

Dec. 1985: Group for Long Term Photometry of Variables.

Jan. 1986: Group for Long Term Photometry of Variables, Lindgren/Ardeberg/Maurice/Prévot L.

Feb. 1986: Lindgren/Ardeberg/Maurice/Prévot L., Group for Long Term Photometry of Variables.

March 1986: Group for Long Term Photometry of Variables.

90 cm Dutch Telescope

Oct. 1985: Gautschy, Courvoisier/Fosbury/Harris/Gry, v. Amerongen/v. Paradijs/Pakull/Pietsch, Pel/de Jong A.

Nov. 1985: Pel/de Jong A.

Dec. 1985: v. Amerongen/v. Paradijs, Lub/de Ruiter, Greve/Georgelin/Laval/van Genderen, Lub/de Ruiter, van Genderen/van Driel.

Jan. 1986: Grenon/Lub.

Feb. 1986: Grenon/Lub, de Zeeuw/Lub/de Geus/Blaauw.

61 cm Bochum Telescope

Oct. 1985: Kieling, Rudolph.

Nov. 1985: Rudolph.

Dec. 1985: Rudolph, Schmidt-Kaler.

Jan. 1986: Thé/Westerlund/Pérez, Schober/Albrecht, Lodén K.

Feb. 1986: Lodén K., Strupat/Drechsel/Haug/Böhnhardt/Rädlein/Rahe, Celnik, Koczet.

List of ESO Preprints (June–August 1985)

374. J. Melnick, R. Terlevich and M. Moles: Near Infrared Photometry of Violent Star Formation Regions. *Revista Mexicana de Astronomia y Astrofisica.* July 1985.
375. A. Tornambè and F. Matteucci: Mass Limit for e-capture Supernovae and Chemical Evolution of Galaxies. *Astronomy and Astrophysics.* July 1985.
376. S. D'Odorico, M. Pettini and D. Ponz: A Study of the Interstellar Medium in Line to M83 from High Resolution Observations of the Nucleus and Supernova 1983n. *Astrophysical Journal.* July 1985.
377. G. Contopoulos and B. Barbanis: Resonant Systems of Three Degrees of Freedom. *Astronomy and Astrophysics.* July 1985.
378. P. Bouchet, J. Lequeux, E. Maurice, L. Prévot and M.-L. Prévot-Burnichon: The Visible and Infrared Extinction Law and the Gas to Dust Ratio in the Small Magellanic Cloud. *Astronomy and Astrophysics.* July 1985.
379. B. Sicardy et al.: Variations of the Stratospheric Temperature along the Limb of Uranus: Results of the 22 April 1982 Stellar Occultation. *Icarus.* July 1985.
380. J. Dachs et al.: Measurements of Balmer Emission Line Profiles for Southern Be Stars. III. New Data and Radial Velocities. *Astronomy and Astrophysics Suppl.* July 1985.
381. C. Barbieri and S. Cristiani: Quasar Candidates in the Field of S.A. 94 ($2^h\ 53^m + 0°\ 20'$). *Astronomy and Astrophysics Suppl.* July 1985.
382. J. Surdej: Analysis of P Cygni Line Profiles: Generalization of the n^{th} Order Moment W_n. *Astronomy and Astrophysics.* July 1985.
383. G. Chincarini and R. de Souza: Optical Studies of Galaxies in Clusters: I. Observations of Hydrogen Deficient Galaxies. *Astronomy and Astrophysics.* July 1985.
384. E.J. Wampler and D. Ponz: Optical Selection Effects that Bias Quasar Evolution Studies. *Astrophysical Journal.* August 1985.
385. J. Melnick, M. Moles and R. Terlevich: The Super Star Cluster in NGC 1705. *Astronomy and Astrophysics Letters.* August 1985.
386. J. Melnick: The 30 Doradus Nebula: I. Spectral Classification of 69 Stars in the Central Cluster. *Astronomy and Astrophysics.* August 1985.
387. R.A.E. Fosbury: Large Scale Ionized Gas in Radio Galaxies and Quasars. Invited paper at "Structure and Evolution of Active Galactic Nuclei". Trieste, April 10–13, 1985. August 1985.
388. G. Vettolani, R. de Souza and G. Chincarini: Isolated Galaxies. *Astronomy and Astrophysics.* August 1985.
389. M.-H. Ulrich et al.: Discovery of Narrow and Variable Lines in the Ultraviolet Spectrum of the Seyfert Galaxy NGC 4151, and an Outline of Our Previous Results. Invited paper at "Structure and Evolution of Active Galactic Nuclei". Trieste, April 10–13, 1985. August 1985.
390. R.H. Sanders: Finite Length-Scale Anti-Gravity and Observations of Mass Discrepancies in Galaxies. *Astronomy and Astrophysics.* August 1985.

The 2nd ESO/CERN Symposium on

Cosmology, Astronomy and Fundamental Physics

will be held at ESO, Garching bei München (F.R.G.),
from 17 to 21 March, 1986

The preliminary programme includes the following topics and speakers:

Neutrino Properties (K. WINTER, CERN, Geneva).
Extragalactic Distance Scale (To be announced).
Cosmic Background Radiation: Observations (F. MELCHIORRI, University of Rome).
The Cosmic Background Radiation and the Formation of Structures (R. A. SUNYAEV*, Space Research Institute, Moscow).
Experimental Status and Prospects of Particle Physics (C. RUBBIA, CERN, Geneva/Harvard University, Cambridge, MA).
Prospects for Future High-Energy Accelerators (S. VAN DER MEER, CERN, Geneva).
High Energy Gamma Ray Sources (To be announced).
Acceleration of High Energy Particles (C. CESARSKY, Observatoire de Meudon, Paris).
Superstrings and Their Cosmological Implications (M.B. GREEN, Queen Mary College, London).
Superdense Matter: Cosmological Aspects (D.N. SCHRAMM, University of Chicago).
Superdense Matter: Laboratory Aspects (K. KAJANTIE, University of Helsinki).
Inflationary Scenarios for the Early Universe (To be announced).
The Age of the Observable Universe in the Inflationary Cosmology (W.A. FOWLER, Caltech, Pasadena).
Distribution of Galaxies and Their Clustering Properties (G. EFSTATHIOU, University of Cambridge).
Particle Dark Matter (J. PRIMACK, University of California, Santa Cruz).
Astrophysical Dark Matter (M.J. REES, University of Cambridge).
Singularities in General Relativity: Possible Astronomical Implications (S. CHANDRASEKHAR, University of Chicago).
Concluding Lecture (D.W. SCIAMA, Oxford University/ISAS, Trieste).

* Participation has not yet been confirmed.

The aim of the symposium is to establish the status of our knowledge on the subject and to provide a forum for discussions among people from different disciplines. To this end about equal time will be dedicated to the formal lectures and to the general discussions on each topic. The audience will be mainly composed of about equal numbers of astrophysicists and particle physicists and will be limited to approximately 150 participants.

The participation in the symposium is by invitation only. People who are definitely interested in participating in the symposium should write to the chairmen of the Scientific Organizing Committee at the addresses below prior to 30 November 1985.

Prof. G. Setti
ESO
Karl-Schwarzschild-Str. 2
D-8046 Garching bei München
F.R.G.

Prof. L. van Hove
CERN
TH Division
CH-1211 Genève 23
Switzerland

Globular Clusters in NGC 3109: Probes for the Study of Galaxy Evolution

E.H. Geyer, Observatorium Hoher List der Universitäts-Sternwarte Bonn
M. Hoffmann, Astronomisches Institut der Universität Münster

Any observer at La Silla who is not working in a telescope control room or watching a movie during a stormy night has the opportunity to see one of the most splendid wonders in the sky without any telescope: Omega Centauri, seemingly a patchy star, but in fact the brightest globular cluster of our Galaxy. Such massive subsystems of a galaxy, each with a

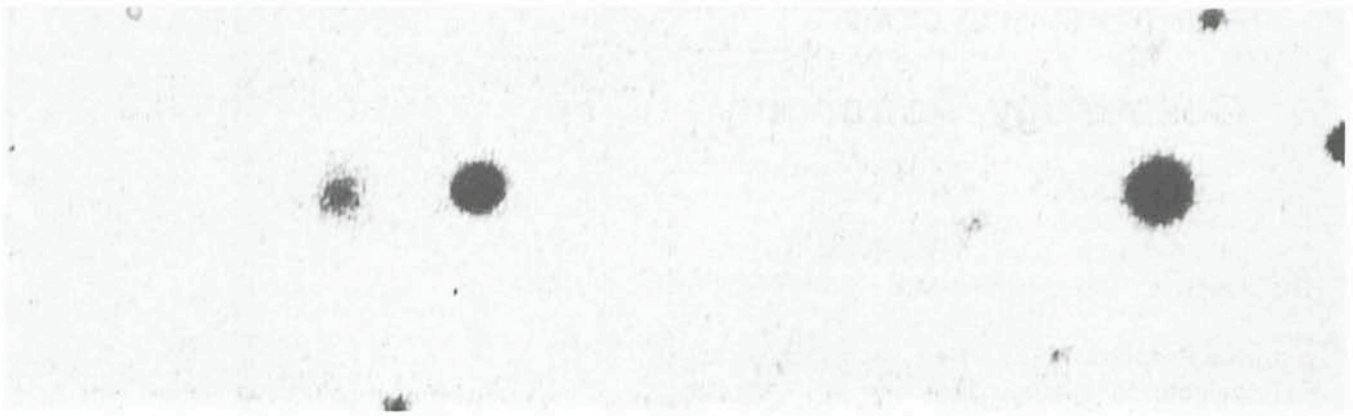

Figure 1: *A two-minute exposure of a globular cluster candidate in NGC 3109, obtained with the CCD camera at the ESO 2.2 m telescope in the V passband. Note the contrast between the fuzzy appearance of this object on the left with the neighbouring star image to its right.*

content of up to a million stars are quite frequent in the universe. We know many thousands of them, most of them around the giant elliptical galaxies of the Virgo cluster of galaxies.

Some Problems

Our own Galaxy possesses at least the 150 globular clusters which were detected up to the present (including doubtful or far outlying objects). From their integrated spectral features it is well known that globular clusters in elliptical or tightly wound spiral galaxies are among the oldest stellar systems we know. In contrast, loosely wound spiral and irregular galaxies like the Magellanic Clouds, contain frequently also luminous and populous star clusters of very young age, but with the typical geometrical structure of the "normal" old globular clusters. Obviously, there is a correlation between the structure of a galaxy and its ability to form globular clusters. Surprisingly, there is no correlation between the mass of a parent galaxy and its content of globular clusters. For example, twice as many globular clusters are known in the tiny Fornax dwarf galaxy as in the ten thousand times more massive giant radio galaxy Centaurus A. Another puzzle may be the location of globular clusters within a galaxy. In galaxies with marked disks the globular clusters are found in a spherical halo around the center of the galaxy. But although there is a clear density gradient with respect to the center, individual clusters with very large mass are observed at large distances from the apparent outer limits of the galaxy. For example the cluster NGC 2419 of our own Galaxy, a quite massive object, has twice the distance from the center of the Galaxy than the Large Magellanic Cloud. Also in the Andromeda galaxy M 31 the brightest known globular cluster has the largest angular distance, far from the region where similar massive stellar aggregates of young objects are found. This is the point to ask (F. Zwicky did that already 30 years ago!) if there are genuine intergalactic globular clusters, and if there is a difference in the internal structure of globular clusters and dwarf galaxies. Dwarf elliptical systems are usually found as companions of giant galaxies and appear tidally stripped in a similar way as the globular clusters. The main difference among them seems to be the surface brightness which is higher for a globular cluster of a given mass by a factor of roughly 100. The only known exception is M32, a companion of the Andromeda galaxy.

These are some of the problems (implicitly connected with those of galaxy evolution) which make the study of galactic and extragalactic systems of globular clusters so interesting. A very important physical parameter for the description of the distribution and interaction of the stellar content of a galaxy bound in globular clusters with the non-cluster content is the angular momentum and its distribution. Typically, a considerable part of the rotational angular momentum of a galaxy is stored in the orbits of the globular clusters. Quite rewarding targets for the study of phenomena related to the complex problem of the formation and evolution of globular clusters and their parent galaxies themselves are dwarf galaxies, because the physical conditions are simpler than in giant galaxies. Some of the evolutionary processes seem to take place on a slower time scale because of the weaker gravitational potential.

The Targets

We started a program of observations of globular cluster systems in nearby dwarf galaxies and selected objects for which no observations for the existence of globular clusters have been carried out. Our main targets were IC 10, a northern irregular object, which just grazes the horizon of La Silla (we observed it from Calar Alto in Spain), and the more southerly placed object NGC 3109, a quite large but to our surprise observationally fairly neglected galaxy of the Magellanic type. This galaxy seems to be just outside the Local Group of galaxies and we see it nearly edge-on. In the first step of our study we searched the available sky surveys for images with condensed but non-stellar appearance in the vicinity of NGC 3109. About half a dozen globular cluster candidates could be isolated. Their images resemble closely those of the major globular clusters of the Andromeda nebula, but smaller in size and integrated brightness on account of the larger distance of NGC 3109. At the end of June 1984 we had the possibility to verify these detections by CCD camera observations with the 2.2 m telescope on La Silla. Although the season for observations of NGC 3109 was quite late and one of the two available nights was cloudy, a few short and a long exposure of two target objects in NGC 3109 could be obtained. The short exposures show them as patches with a smooth intensity profile of round shape (Fig. 1), and the long exposure images appear only slightly more extended. Also the outermost parts of the latter images are not resolved into stars, but their patchy appearance resembles the statistical distribution of stars which is typical for globular clusters as can be seen on photographs e.g. of the bright galactic globular cluster M5. Though there are morphological differences between giant elliptical galaxies and globular clusters, it cannot be excluded that an apparent globular cluster of a nearby

galaxy is confused with a distant background elliptical galaxy. The easiest way of distinction would be the measurement of the radial velocities of the relevant target objects. However, the nature of the found objects is much better established, and they are quite probably genuine globular clusters of NGC 3109: Their colours are moderately red, and we think they are normal halo objects of this galaxy. This is supported by their distant position from the main disk of NGC 3109.

Unfortunately the other cluster candidates of NGC 3109 could not be observed during this observing run. But the remainder of the observing time was used to observe some other nearby galaxies. A very interesting galaxy turned out to be the probably outlying member of the Sculptor group of galaxies A0142-43. In its halo two objects were observed which resemble those of the found globulars in NGC 3109, and may be even a bit larger in their absolute dimensions. Again, their position relative to the parent galaxy and their colours indicate typical halo objects. A huge HII region in the main body of A0142-43 shows that star-forming processes took place quite recently in it.

If there are populous clusters of very young age associated with it they are veiled by this bright gas complex. It should be noted that the estimated absolute luminosity of A0142-43 is 1.5 magnitudes fainter than that of the Small Magellanic Cloud.

We can conclude that our observations tend to confirm the complex situation among the galaxies and their cluster systems. Although it may be useful to detect new cluster systems, the relevant information of their role among the evolution of galaxies can certainly much better be found in detailed kinematical studies.

Chromospheric Modelling in Late-type Dwarfs 2. CES Observations of Active and Quiescent Stars

B.H. Foing, ESO
J. Beckman, Instituto de Astrofísica de Canarias
L. Crivellari, Osservatorio Astronomico di Trieste
D. Galleguillos, Universidad de La Serena and Max-Planck-Institut für Radioastronomie, Bonn

1. Introduction

For many years it has been accepted that a stellar atmosphere cannot be considered as a closed thermodynamic system isolated by notional adiabatic walls, and without exchange of matter with the surrounding interstellar medium. A detailed exchange of ideas, developed earlier by Pecker, Praderie and Thomas (1973, *Astron. and Astrophys.*, **29,** 283) can be found in Thomas' monograph "Stellar Atmospheric Structural Patterns" (1983, NASA SP – 471).

Twenty years of UV observations from space have given us clear evidence that stars in every part of the HR diagram are losing mass, and that their external layers are heated by non-radiative energy fluxes up to coronal temperatures of several millions of Kelvins. These major departures from conditions of equilibrium make the modelling of a stellar atmosphere a more difficult task. In fact, the computation of detailed models for the solar and stellar atmospheres is even more difficult than the corresponding problem for photospheres. As discussed in the first article (*The Messenger,* **38,** p. 24), chromospheric models must take into account not only the severe departures from LTE and radiative equilibrium, but also the increased importance of magnetic fields in controlling the energy transport, as well as the linked horizontal inhomogeneities in density and temperature. The most valuable observations available for constraining model chromospheres are high resolution spectra of the lines of the most abundant elements, especially Hα, the H and K lines of CaII, the infrared triplet of CaII, and the h and k lines of MgII.

In this paper we shall describe the observations that we have obtained for a sample of active and quiescent late-type dwarfs as an input for chromospheric modelling. We describe briefly the background of the program originating in IUE observations of MgII lines, and the objectives of our complementary observations of chromospheric lines at ESO. From the spectra obtained with the Coudé Echelle Spectrograph (CES) we have derived preliminary spectroscopic indicators of activity. We show how this empirical approach can provide a guideline for the next phase of our program: quantitative line modelling from which should emerge the temperature structure, the energy balance, and the structure of the heterogeneity of late-type chromospheres.

2. IUE Observations of MgII Lines, and the Background to the Program

During the past six years we have been observing a representative sequence of late-type (late F and G) dwarfs using the high resolution spectrograph of IUE to obtain high quality profiles of the h and k lines. As described in article I, an almost serendipitous consequence of the failure of the stars to show reasonable variability has been a set of averaged profiles of very high quality, with spectral resolution of 1.8×10^4, high enough to resolve the Doppler self-absorbed parts of the core, and signal to noise ratio of 30 even in the hI and kI minima, good enough for model fitting. Thanks to the powerful IUEARM set of data reduction programs we have been able to identify and remove the interstellar MgII, leaving line shapes which reflect intrinsic chromospheric and photospheric processes. In addition, absolute fluxes in MgII have been obtained for comparison with theoretical predictions.

These predictions are of two types. One concerns the way in which energy is deposited within the chromosphere: whether by acoustic or magneto-acoustic input. This we can examine through a comparison of line profiles with model atmospheres. The second is the relation between age, rotation rate and chromospheric activity, first quantified by Wilson (*Ap. J.*, 1980: **226,** 379) and subsequently explored observationally by Vaughan and his co-workers. Activity indicators can be derived from spectra, calibrated in a coherent manner, and studied for variations in effective temperature, rotation rate and age. In a second step the line profiles can be modelled in detail. An intrinsic weakness of any chromospheric model based on

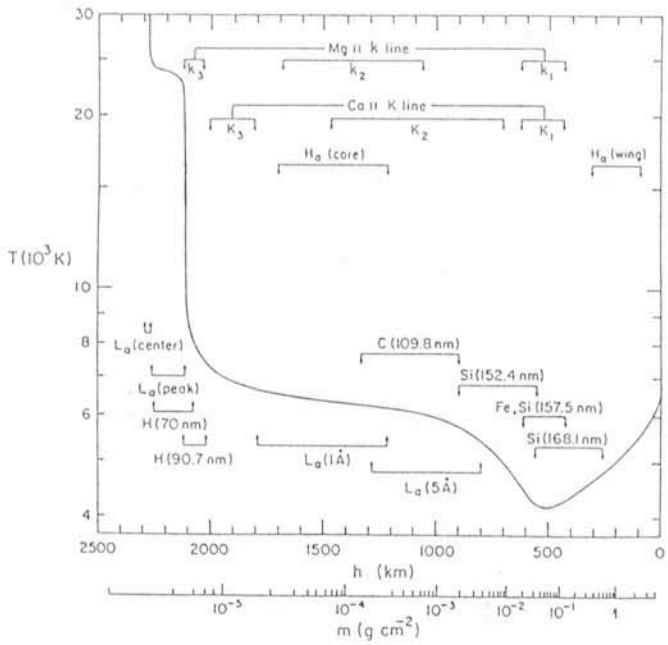

Figure 1: *On the average quiet-Sun temperature distribution derived by Vernazza, Avrett and Loeser (1981)* Ap. J. Suppl. **45,** *635, the estimated depths where the various spectral features originate are indicated for the Mg II, Ca II and Hα lines.*

fitting a single emission line is its non-uniqueness. This is one important reason to use the group of lines referred to in the introduction, where profiles are formed in different, but thoroughly overlapping layers of the chromosphere. In Figure 1 we indicate the mean formation layers of the core and the wings of those lines for the Sun, i.e. for the quiet Sun temperature distribution derived from the EUV continuum, Lyα and other observations by Vernazza, Avrett and Loeser (*Ap. J. Suppl.* 1981: **45,** 635)

3. Objectives of our Chromospheric Modelling Programs

Clearly the most striking difference between the chromospherically active and chromospherically quiescent stars as far as our data are concerned is the fact that the Mg II emission cores do not exhibit major quantitative differences, whereas the Ca II cores are strikingly different, with the active stars showing much more emission.

In one sense the reasons for these chromospheric differences are fairly clear, as we know that the active regions of the type observed on the Sun (where the chromospheric plages show up strongly in Ca H and K) are likely to be the cause of the H and K enhancements in active stars. Solar plage activity corresponds to magnetic activity and hence strong stellar Ca H and K corresponds to stars with greater average surface magnetic activity. One result of this activity is to channel more energy into the chromosphere, possibly via MHD waves, and a major manifestation of the activity is the enhanced presence of magnetically controlled jets, or spicules, which are concentrated along the boundaries of the supergranules in the solar chromosphere (spicules have diameters in the 10^3 km range, and the supergranules in the 10^4–10^5 km range), and which appear with greater surface density in the plages. Put simply, the quiescent resonance line emission cores exhibit the interspicular chromosphere, and the active cores exhibit the spicular component, although this is an oversimplification.

Any chromospheric model must take into account this inhomogeneity, although it is possible that even two stream models will prove insufficient. At all events, the ability to obtain the highest quality profiles, with a spectral resolution sufficiently high that a resolved element is significantly finer than the sharpest core features, is allowing us to make progress in the following areas:

(a) To measure true chromospheric radiative losses as a function of T_{eff} and rotational velocity, making comparisons between acitve and quiescent stars.

(b) To assess the run of microturbulent velocity with depth in the chromosphere.

(c) To compute numerically departures from hydrostatic equilibrium, by using measured line core asymmetries to assess the velocity fields.

(d) To attempt detailed models in which all the parameters of a chromosphere can be derived, using the modern analytical tool of partial redistribution theory, and taking both horizontal inhomogeneity and velocity fields into account.

In addition to high resolution CES spectra on which the empirical side of a modelling program is now being based, it is important to have three other types of information at our disposal: (a) absolute spectrophotometry at modest resolution, in order to calibrate fluxes; (b) near infrared photometry in the classical I, J, H, K bands in order to derive the major radiative loss contribution made by H^- in these cooler stars, and (c) if practicable, direct measurements of rotational modulation of (eg. H and K) line cores because this is the only accurate way to infer rotational velocities of slowly radiating stars (v sin i $\lesssim$2 km s).

4. The Use of ESO Facilities

There is no doubt that the CES spectrograph, fed either by the CAT or of course by the 3.6 m telescope, is the leading coudé facility at present available. In our recent runs, aimed at acquiring the line profile data whose purpose is outlined above, we have obtained at Hα, for 3rd magnitude stars, signal-to-noise ratios of 300 in the continuum, with spectral resolution 10^5, in exposures of the order of 1 hour with the CAT. When one considers that the free spectral range of between 30 Å and 70 Å is adequate to take in even the broadest photospheric absorption and that the reticon offers a dynamic range capable of measuring the H1 and K1 intensity minima at the same time as the H2 and K2 maxima, there is no further need to emphasize the value of this facility for chromospheric modelling observations. We have now sampled 13 quiescent and 12 active stars, taking in all of the chromospheric diagnostics mentioned, plus the $^6Li/^7Li$ doublet at λ 6707 Å for most of them. They cover a range of spectral classes from F8 to K5 down to limiting magnitude $m_v = 5$. At this magnitude one is beginning to touch, with the CAT and the present instrumental configuration, effective dark count limitations on the signal-to-noise ratio required to sample the H1 and 1k minima.

In addition to the CES, ESO offers the near-infrared standard photometer needed to compute the H^- radiative loss measurements with those of the two other major contributors, viz. the Mg II and Ca II resonance doublets. Further the use of the 1.5 m telescope with Boller and Chivens spectrograph for making absolute flux determinations provides another key link in the chain of observational inferences needed for useful chromospheric modelling. In fact, only the UV spectra (Mg II and Lyα) and the direct measurement of rotational velocity via H and K modulation are lacking at present in order to complete the battery of facilities required to attack this problem. While it will never be possible to do away with IUE or ST, it would indeed be possible to envisage a rotational modulation spectrometer attached to an ESO telescope of the 1.5 m class.

Even now, the less accurate approach to rotational velocities via line asymmetries can be used on CES spectra. In sum, ESO is certainly currently the best observatory in the world from which to mount a concerted campaign on chromospheric activity of solar-like stars.

5. Comparison of Observed Chromospheres Inferred from CES Spectra

As examples of the comparison of chromospheric lines from pairs of stars with similar spectral type but with different bands of activity we show, in Figure 2a and 2b, CES spectra of the cores of the CaII H lines in ε Eri and α Cen B. The K1 V star α Cen B shows a central reversal which is in fact quite clear when contrasted with the underlying photospheric background. However, α Cen B can be considered as a quiescent star compared to the K2 star ε Eri, for which the very strong central emission indicates a much higher degree of activity. Note also the asymmetry between the H2 violet and red peaks, as well as the appearance of the Balmer line Hα in emission for ε Eri. The CaII core of ε Eri looks similar to the cores of these lines emitted from a plage region on the Sun. We can use the other chromospheric lines in addition to the classical K or H indexes, to study the differential effect of the acitivity.

Figures 3a and 3b show spectra of Hα for the two K2V stars ε Eri end O^2 Eri. The wings of the Hα profiles are undistinguishable for the two stars, which confirms that they have the same effective temperature. However, the intensity at the center of the core of the active star ε Eri is 40% more than for the quiescent O^2 Eri. The difference in the equivalent width between the two profiles represents the energy excess contribution in Hα due to the activity. Note here the slight asymmetry in the core of Hα for ε Eri.

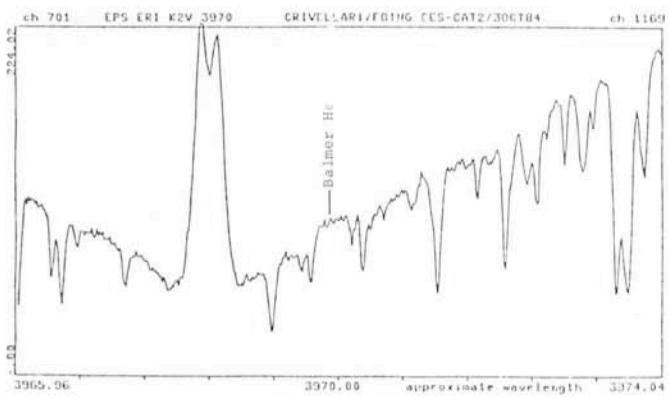

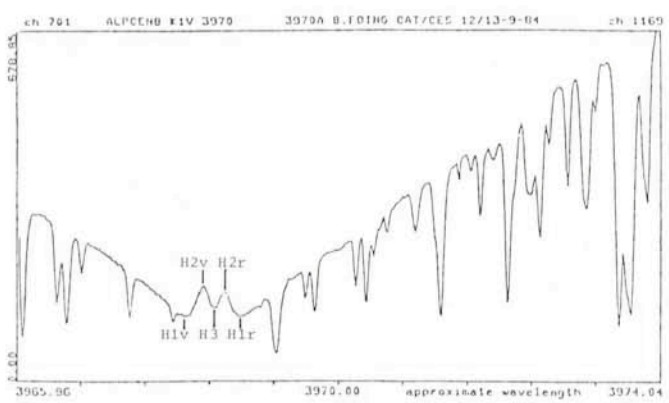

Figures 2a and 2b: *Quick-look spectra of the core of the CaII H line for the stars ε Eri (K2V) and α Cen B (K1V). The central reversal appears clearly by contrast with the underlying photospheric background, even for the quiescent star α Cen B. The very active ε Eri shows a central emission very similar to that emitted from the solar "plages".*

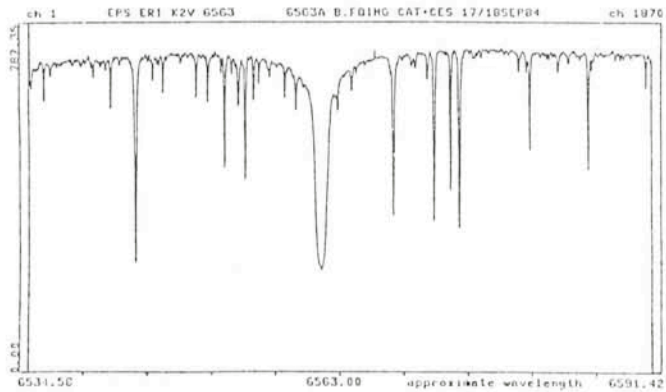

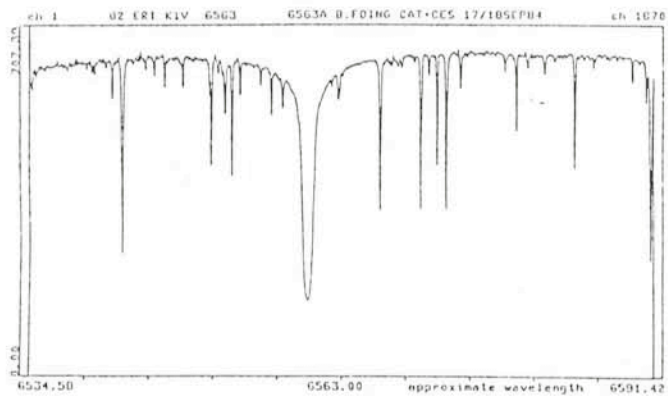

Figures 3a and 3b: *Spectra of the Hα line for the two K2V stars ε Eri and O^2 Eri. The wings of the Hα line are undistinguishable between the two stars, but the core intensity of the active ε Eri is 40 % more than for the quiescent O^2 Eri, showing the chromospheric emission due to the activity.*

For the same two stars, Figures 4a and 4b show spectra of two of the Ca infrared triplet lines. Here again we can see clearly that the absorption lines are filled in by a chromospheric emission component; the intensities at the centers of the two lines are twice as strong in ε Eri as in O^2 Eri. In order to use these observations as measurements of flux excesses we must proceed via absolute flux calibrations, a consideration which clearly applies to all our measurements. Once again in these triplet lines there is asymmetry in the core emission, and also clear evidence not only of emission, but of a sharp central self absorption. It is interesting to note that we have found in the more active stars changes in the central intensity and in the asymmetry of the chromospheric lines. These changes could be related to rotational modulation of the chromospheric emission due to plage transit over the visible surface. In these cases we have to ensure that a complete set of spectral lines, either simultaneous observations or observations at the same rotational phase, are taken, if we intend to produce consistent models of active chromospheres.

6. Activity Indicators

In section 5 we illustrated some spectral signatures of the activity observable via the CES in different lines. Here, in Figure 5, we have plotted a group of activity indicators. Namely the core intensity in the line of Hα and of the "triplet" lines at

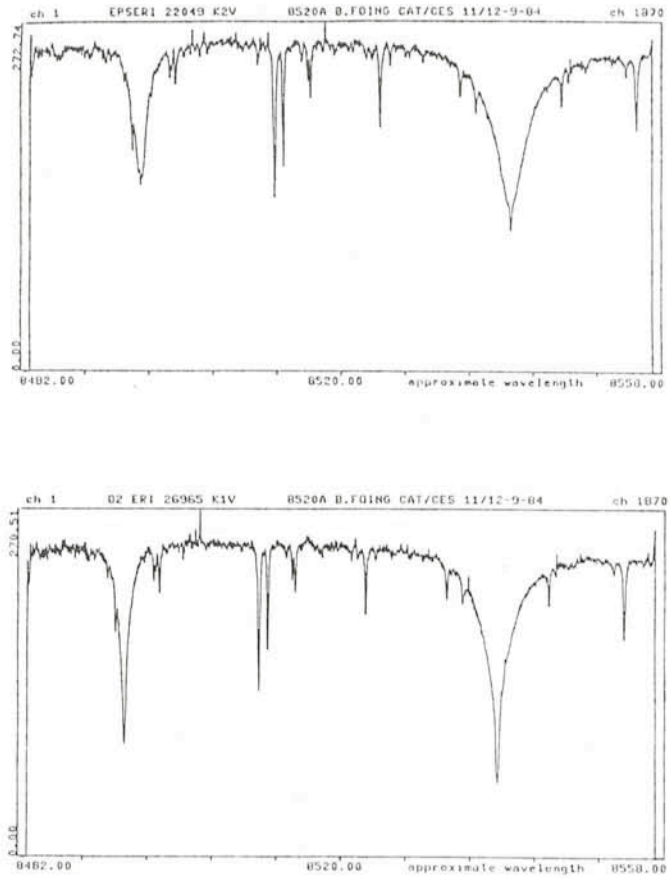

Figures 4a and 4b: *Spectra of two lines of the Ca infrared triplet at 8498 and 8542 Å, for ε Eri and O^2 Eri. Again, for the active ε Eri, the Ca II absorption lines are partially filled by a chromospheric emission core.*

λ 8490 and λ 8542. These intensities are presented in units of flux in the nearby continuum. Although still somewhat crude, these indicators are able to give us some useful immediate information about stellar activity. The most notable feature of Figure 5 is the wide dispersion of activity with spectral type, which is certainly consistent with the existence of another parameter controlling the activity. This is probably the rotation rate, as suggested by Vaughan et al. (*Ap. J.*, **250,** 276, 1981). We have included our sample of quiescent stars in Figure 5 to provide a baseline from which activity can be measured and by way of contrast have also included indicators for two RS CVn binaries, which are known to show very high levels of activity.

These rough activity indicators can be refined to represent by calibration true chromospheric losses in the corresponding lines. They are useable as guidelines to describe the variety of chromospheres of our star sample, and will be employed in plots against effective temperature and rotation period. Subsequently we will, however, need to make detailed models, deriving the temperature structure and energy balance with height, which are necessary to analyze the processes which in fact heat the chromosphere.

7. Conclusion

Observations of quiescent and active stars to date have resulted in clear analogs to the activity phenomena observed on the Sun: active regions, photospheric spots, chromospheric plages, coronal structures. Leading directly from the work originally carried out for the Sun by Lemaire et al. and by Vernazza, Avrett and Loeser, our observations can provide strong constraints on models of stellar chromospheres. In a third paper of this series for the *Messenger* we shall present an analysis of subsurface structures linked with activity mecha-

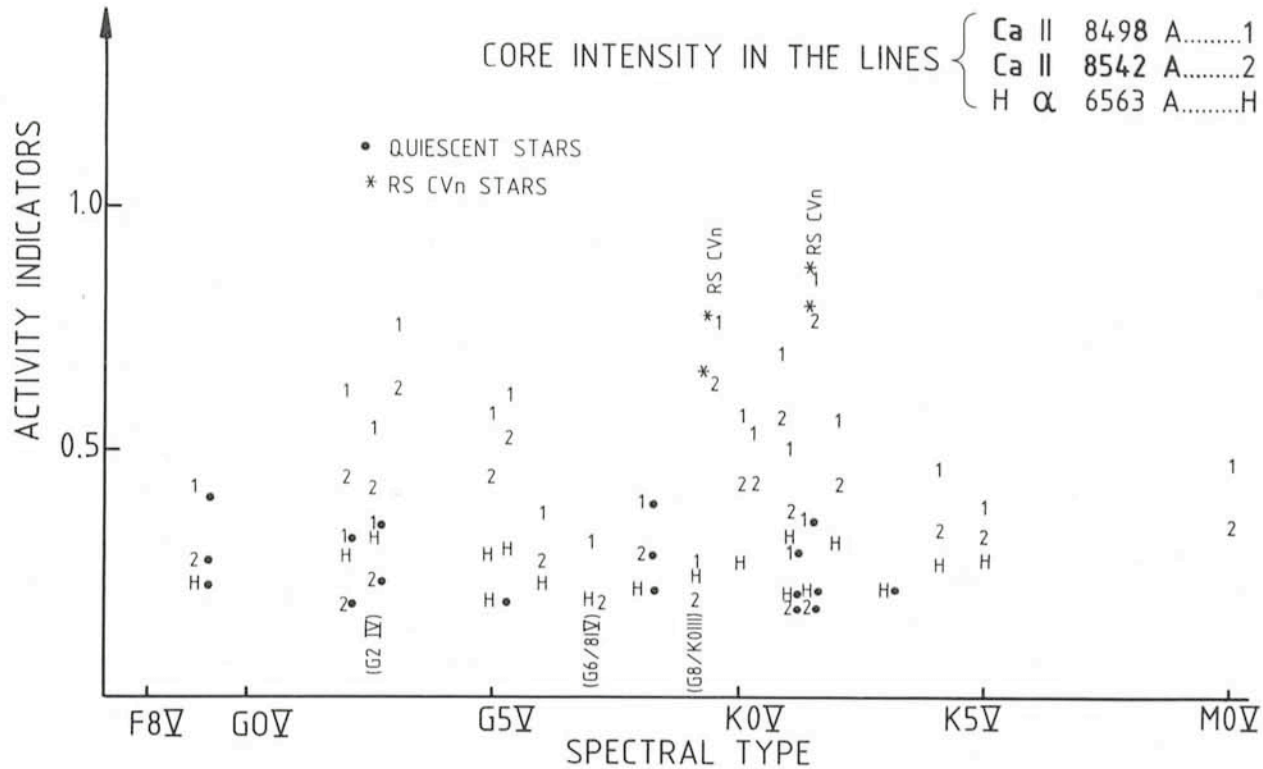

Figure 5: *Variation of some activity indicators as the core intensity of Hα (marked H) and of 8498 Å and 8542 Å lines of the Ca II infrared triplet (marked 1 and 2) for our sample of late type dwarfs. The continuous underlying envelope for our sample suggests a quiescent reference for the study of the activity.*

nisms (magnetic fields and energy sources), gleaned from evidence of spectral line changes during the rotational modulation. We want to understand how the chromospheric structure and magnetic heterogeneities behave according to the major stellar parameters, viz. mass, age, composition and rotation rate, and the present observations will provide us with a key to understanding both chromospheric heating mechanisms, and the dynamo mechanism in late-type stars.

The Increasing Importance of Statistical Methods in Astronomy

A. Heck, Observatoire Astronomique, Strasbourg, France
F. Murtagh, The Space Telescope European Coordinating Facility, European Southern Observatory*
D. Ponz, European Southern Observatory

> You may ask:
> "What can a hard headed statistician offer to a starry eyed astronomer?"
> The answer is:
> "Plenty."
>
> Narlikar (1982)

Generalities

In the past, astronomers did everything individually, from the conception of a project to the collection of data and their analysis. As the instrumentation became more complex, teams had to be set up and they progressively included people (astronomers or otherwise) specialized in technology. Today it is practically impossible to run a project at the forefront of astronomical research without the help of these technologists.

In a similar way, one can already see that, at the other end of the chain, teams will have to include also people specialized in methodology to work on the collected data. And we are not thinking here only of image processing (which is a natural consequence of sophisticated technology), but mainly of a methodology applicable to already well-reduced data. This is actually the only way to face the challenge put to us by the accumulation of data.

Compared to the past, we are indeed collecting now a huge amount of data (see e.g. Jaschek, 1978), and the rate will speed up in the next decades. Just think that the Space Telescope will send down, over an estimated lifetime of 15 years, the equivalent of 14×10^{12} bytes of information, which means a daily average of 4×10^{9} bytes! But even if we exclude this special case of ST, we have now at our disposal more and more instruments which are collecting observations faster and faster. And these data are more and more diversified. The rate of data accumulation is higher than the rate of increase of the people able to work on them.

Thus, we will have to work on bigger samples if we want to take advantage and fully use the information contained in all these data, globally and individually. We might well live at the end of the period when a significant number of astronomers are spending their lives investigating a couple of pet objects. If not, what would be the use of collecting so many data?

One way to work efficiently on large samples is to apply, and if necessary to develop, an adequate statistical methodology. If Nature is consistent, the results obtained by applying the tools developed by the mathematicians and the statisticians should not be in contradiction with those obtained by physical analyses.

However, do not let us say what we did not say: the statistical methodology is not intended to replace the physical analysis. It is complementary and it can be efficiently used to run a rough preliminary investigation, to sort out ideas, to put a new ("objective" or "independent") light on a problem or to point out sides or aspects which would not come out in a classical approach. A physical analysis will have anyway to refine and interpret the results and take care of all the details.

Probably the most important statistical methods, for astronomical problems, are the multivariate methods such as Principal Components Analysis (PCA) and Cluster Analysis. The former allows the fundamental properties to be chosen for a possibly large number of observational parameters. This is clearly an important task, since the apparent complexity of a problem will necessarily grow with improvement in observational techniques.

The problem of clustering is that of the automatic classification of data. Clustering methods can also be employed to pick out anomalous or peculiar objects. These techniques all work at will in a multidimensional parametric space, while graphically, and also classically in statistics, it is difficult to get results from more than two dimensions. These statistical methods are often considered as descriptive rather than inferential and, since astronomy is fundamentally a descriptive science, they would appear to be ideally suited for problems in this field.

In the same way that instrumentation should not be employed without respecting its conditions of use, algorithms should not be applied as black boxes by non-specialists without paying attention to their applicability constraints and their result limitations. Forgetting this golden rule is the best way to contribute to the bad reputation of statistics while ruining from the start any attempt at elaborating relevant conclusions.

Maybe somewhat paradoxically, astronomers have not been among the quickest to realize the potentialities of the "modern" statistical methodology. One of us (AH) became interested in 1974–75 and produced among the first papers in the field. But the idea was in the air and applications started to multiply. He therefore suggested the holding of a first meeting on "Statistical methods in astronomy". It took place in September 1983 at Strasbourg Observatory with the European Space Agency as co-sponsor (the proceedings were published as ESA SP-201).

This was the first opportunity to bring together astronomers using various statistical techniques on different astronomical objects and to review the status of the methodology, not only among astronomers, but also with invited statisticians. The

* Affiliated to the Astrophysics Division, Space Science Department, European Space Agency.

colloquium was a real success and another one is planned, most likely in 1987. In addition, a working group, concerned with the application of statistical methodology to astronomical data, is being set up. A newsletter should keep interested persons in touch and informed of the various activities in the field.

We shall present in the following a few examples of applications which do not exhaust all the possibilities and can only give a partial idea of the variety of the problems that can be tackled with this methodology.

Photometry Versus Spectroscopy

Since practically nothing had been done when AH started working in the field, he was first concerned with the applicability of this "modern" statistical methodology to astronomy. Thus he decided to put the algorithms on the trial bench of stellar data because there were a lot of such data available and because the corresponding physics was well established (and could be efficiently used for comparison).

A priori, however, it might be more appropriate to apply this methodology to non-stellar objects because their physics is less developed and because the data are more heterogeneous, incomplete, very diverse (continuous, discrete, binary, qualitative, . . .) and are thus challenging for the methods.

In stellar astronomy, an interesting subject was to study the interface between photometry and spectroscopy, especially in the framework of stellar classification. In the past, photometric and spectroscopic data were thought of as conflicting by some astronomers, but today most consider these techniques to be complementary. With P. C. Keenan (1973), we now "take it as evident that the aims of stellar classification are the same whether we work by direct photoelectric photometry through filters, by spectrophotometry, or by visual classification of spectrograms".

How well could, for instance, photometric indices of a star allow us to predict its spectral classification? Apart form its scholastic interest, this question has direct practical observational implications since photometric colours are much more quickly collected than good spectrograms, and with a smaller instrument for a given object.

The first step (Heck, 1976) has been to point out by multivariate statistical algorithms the most significant indices or group of indices in the *uvby* β photometric system for different ranges of spectral types. The photometric catalog (Lindemann & Hauck, 1973) was considered as a set of numerical data and the only physical hypothesis which intervened was a correlation between the effective temperature and the spectral types. The results were in full agreement with those of Strömgren (1966, 1967) obtained by physical analysis. The correct indices or groups of indices were selected as discriminators of luminosity and effective temperature.

The second step (Heck et al., 1977) was to directly confront photometric and spectroscopic data by applying clustering algorithms in an adequate multivariate space to the photometric indices of the same catalog (considered again purely as a set of numerical data). Then looking at the continuity of the arborescences or the homogeneity of the groups obtained from the point of view of the spectral classification, it transpired that about 8 % of the stars where deviating significantly from the ranges in spectral types and luminosity classes they should naturally belong to. These discrepancies resulted either from a wrong spectral type (as some re-determinations indicated), from poorly determined photometric indices, or simply because photometric indices, even when well selected, give information of a type different from the spectral features, and also from different wavelength coverages.

Might this mean that spectral classifications could be predicted from *uvby* β indices with about 90 % chance of being correct? This was investigated in a couple of subsequent papers (Heck and Mersch, 1980; Mersch and Heck, 1980) by elaborating an algorithm involving isotonic regression (working on the ranks of the spectral subtypes and luminosity classes) and stepwise multiple regressions (selecting the most significant indices or combinations of indices).

It resulted that there was an 80 % chance of predicting the spectral type within one spectral subtype for luminosity classes I to IV and an 87 % chance for luminosity class V. As far as luminosity was concerned, there were 44 %, 28 % and 56 % chances of predicting it correctly for luminosity classes I, III, and V respectively. This might point out some inability of the *uvby* β photometry *alone* to discriminate properly the luminosity and it would be worthwhile to undertake a similar study with different photometry.

Ultraviolet Spectral Classification

The previous investigations were more centered on studying the applicability of the "modern" statistical methodology to astronomical data than on tackling new fields. An opportunity came recently with the classification of IUE low-dispersion stellar spectra.

The International Ultraviolet Explorer (IUE), launched on 26 January 1978 and still operating in an observatory mode, is the most successful astronomical satellite up to now. Details can be found in Boggess et al. (1978a and b). We shall only recall here that it is collecting low- and high-resolution spectra of all kinds of celestial objects in the ultraviolet wavelength range (UV) covering about 1150 to 3200 Ångströms.

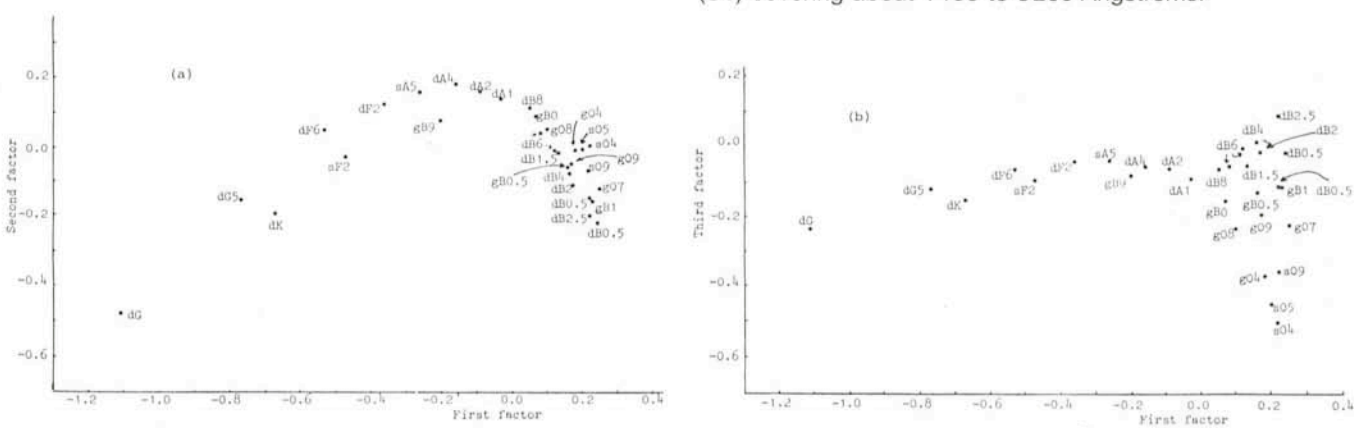

Distribution of the group barycenters in the plane of the first two PCA factors (a) and of the first and third PCA factors (b) derived from the IUE spectral data. Each center has been named according to the spectral mode in the multivariate space of the first twenty PCA factors. The UV spectral symbols have been introduced in Heck et al. (1984).

From earlier work on data collected by the S2/68 experiment on board the TD 1 satellite, it had been shown that stars which are spectrally normal in the visible range do not necessarily behave normally in the ultraviolet range and vice versa (see Cucchiaro et al., 1978, and the references quoted therein). Consequently, MK spectral classifications defined from the visible range cannot simply be extrapolated to the UV.

A UV stellar classification program, supported by a VILSPA workshop on the same subject (proceedings published as ESA SP-182) was then initiated in order to define from IUE low-resolution spectra smooth spectral sequences proper to the UV and describing the stellar behavior in the UV while staying as far as possible in accordance with the MK scheme in the visible.

The first volume of a reference atlas has been produced (Heck et al., 1984), together with reference sequences and standard stars. The considerable underlying classification work has been carried out following a classical morphological approach (Jaschek and Jaschek, 1984) and it essentially confirmed that there is no one-to-one correspondence between the UV and visible ranges.

Stellar spectral classifications are more than taxonomical exercises aiming just at labelling stars and putting them in boxes by comparison with standards. They are used for describing fundamental physical parameters in the outer atmosphere of the stars, to discriminate peculiar objects, and for other subsidiary applications like distance determinations, interstellar extinction and population synthesis studies.

It is important to bear in mind that the classification systems are built independently of stellar physics in the sense that they are defined completely by spectral features in selected standards in a given wavelength range (see e.g. Jaschek, 1979, and Morgan, 1984). If the schemes are based on a sufficiently large number of objects, it appears easily that they are intimately linked with the physics, but not necessarily of the same stellar regions if they refer to different wavelength ranges. Consequently, the discrepancies reported between the MK system and the UV frames are not too surprising.

Moreover, the only way to confirm independently the correctness of the UV classification frame introduced in the atlas was to remain in the same wavelength range. Therefore, statistical algorithms working in a multidimensional parametric space were applied to variables expressing, as objectively as possible, the information contained in the continuum and the spectral features (Heck et al., 1985). This was done through, on the one hand, an asymmetry coefficient describing the continuum shape and empirically corrected for the interstellar reddening, and, on the other hand, the intensities of sixty objectively selected lines (which included all the lines retained as discriminators in the atlas).

These line intensities were weighted in a way we called the "variable Procrustean bed method" because, contrary to a standard weighting where a given variable is weighted in the same way for all the individuals of a sample, the spectral variables were weighted here according to the asymmetry coefficient which varies with the star at hand. The algorithm applied to the set of the variables consisted of a Principal Components Analysis and a Cluster Analysis.

The individual classifications resulting from the morphological approach used for the atlas were fully confirmed, and ipso facto the discrepancies with the MK classifications in the visible range. The groups resulting from the Cluster Analysis displayed good homogeneity and an excellent discrimination for spectral types and luminosity classes, especially in the early spectral types which were well represented in the sample used for this study. The standard stars are located in the neighborhood of the barycenters of the groups (see figure).

Currently the contributions of the successive principal axes resulting from the Principal Components Analysis are being investigated in greater detail, and we are looking forward to including more data from the IUE archive in order to refine the conclusions.

Star and Galaxy Separation

Survey work on many plates rapidly encounters problems of processing very large numbers of objects. One current theme of research is to simplify the carrying out of, and make use of the results of, such surveys as the ESO/Uppsala survey of southern galaxies (see Lauberts and Valentijn, 1983). Firstly, the use of multivariate methods in classifying data derived from images is being studied; and secondly, novel approaches are being looked at for the classification of galaxies. In this section, we will look at each of these in turn.

In discriminating between objects on survey plates, the first question which arises is the choice of parameters to extract. At present the object searching algorithm in MIDAS outputs information regarding 20 variables for each object found. Using Prinicpal Components Analysis easily allows it to be seen if all of these variables are necessary – in fact, we have usually found that about 2 or 3 variables (e.g. isophotal magnitude, relative gradient) are sufficient. These provide approximately as much "information" as the original set of variables. For classifying the objects into the major classes (i.e. stars, galaxies, plate defects), the usefulness of the 20-odd variables produced at present is being investigated. We are considering other shape parameters, such as the moments, and hope to be shortly in a position to suggest to the user a sequence for carrying out an analysis such as the following: choose a particular set of variables to characterize the objects studied; run this through a Principal Components Analysis in order to arrive at a best-fitting pair of variables (a linear combination of those chosen) which can be plotted and studied; then use these as input to a clustering program in order to determine the major groups of objects present. Such an approach will never replace the expert (consider for example the range of variables which are candidates for star/galaxy discrimination, and some of which are reviewed by Kurtz, 1983); however, in providing useful analytic tools, it can increase the performance of the expert and indicate to him/her further interesting aspects which would not have been appreciated if overshadowed by the sheer quantity of data to be analyzed.

The large quantity of data, of course, in itself demands the provision of increasingly automated means of analysis. Progress in an expert system to determine galaxy types (Thonnat, 1985) will probably always be hampered by large computational time requirements if sophisticated pattern matching algorithms are not at the core of such systems. Therefore, it is being attempted to assess the potential for classifying galaxies – at least into the major types – by using for each galaxy its magnitude versus surface brightness curve (see Lauberts and Valentijn, 1983). A novel curve matching technique has been developed, a measure of similarity thereby determined, and a clustering carried out on the basis of such similarities. Results obtained so far (Murtagh and Lauberts, 1985) show consistency with a human expert's classification into ellipticals and spirals.

Statistical Algorithms in MIDAS

In the current version of MIDAS we have included commands for some of the basic methods of multivariate statistical analysis. The data matrix is structured as a table where the different objects are associated with rows and the variables

are associated with columns. The methods currently available are:

– Principal Components Analysis, to produce the projection of the data matrix onto the principal axes.

– Cluster Analysis, using hierarchical clustering with several agglomerative criteria (single link, complete link, minimum variance, etc.).

– Fast iterative non-hierarchical clustering methods.

In this context, the tables in MIDAS provide a bridge between the raw data and the algorithms for analysis. Data originally in the form of images or catalogs can be put into the analysis program by structuring the extracted information as tables, a natural way of representing the objects in the parameter space.

These commands are in an experimental state. Work is ongoing in making more statistical methods available within the interactive framework of MIDAS. Special attention will be given to the friendliness of usage by means of display facilities and easy interaction. Unlike many statistical packages commercially available, MIDAS offers the advantage of integrating image processing algorithms with extensive graphics capabilities and, of course, the statistical methods.

The linking-up of data collection and of statistical data analysis – of database creation and of an important use to which a database is put – is also of singular importance. The future existence of an ESO and of a Space Telescope archive creates exciting possibilities for the possible use of multivariate statistical procedures on a large scale. A step of far-reaching implications was taken a few years ago when the large-scale archiving of data was linked to the down-stream analyzing (by multivariate statistical methods) of such data: this was when Malinvaud, head of the French statistical service (INSEE), strongly linked the two together (Malinvaud and Deville, 1983). Multivariate statistical analysis of data requires that the data collection be competently carried out; and, in return, it offers the only feasible possibility for condensing data for interpretation if the data is present in very large quantities.

A Collaborative Future

Current trends in astronomical research not only create prospects for statistical methods to be used, but for reasons mentioned in this article they require them. The flow will not be just one-way however: statisticians will also learn from the problems of astronomy. Computational problems related to the large amounts of data which must be handled, the best ways to treat missing values and mixed qualitative-quantitative data, and even the most appropriate statistical methods to apply – all these and many more currently unforeseen issues will lead to a very fruitful and productive interaction between methodologist and astronomer over the coming years.

References

Boggess, A. et al. 1978a, *Nature* **275,** 377.

Boggess, A. et al. 178b, *Nature* **275,** 389.

Cucchiaro, A., Jaschek, M., Jaschek, C. 1978, *An atlas of ultraviolet stellar spectra,* Liège and Strasbourg.

ESO 1985, MIDAS Operating Manual No. 1.

Heck, A. 1976, *Astron. Astrophys.* **47,** 129.

Heck, A., Albert, A., Defays, D., Mersch, G. 1977, *Astron. Astrophys.* **61,** 563.

Heck, A., Egret, D., Jaschek, M., Jaschek, C. 1984, IUE low-dispersion spectra reference atlas. Part 1. Normal stars. ESA SP-1052.

Heck, A., Egret, D., Nobelis, Ph., Turlot, J.C. 1985, Statistical classification of IUE low-dispersion stellar spectra, in preparation.

Heck, A. and Mersch, G. 1980, *Astron. Astrophys.* **83,** 287.

Jaschek, C. 1978, *Q.J. Roy. Astron. Soc.* **19,** 269.

Jaschek, C. 1979, in *Classification Spectrale,* Ecole de Goutelas, ed. D. Ballereau, Obs. Meudon.

Jaschek, M. and Jaschek, C., 1984, in *The MK Process and Stellar Classification,* ed. R.F. Garrison, David Dunlap Obs., p. 290.

Keenan, P.C. 1973, in *Spectral Classification and Multicolour Photometry,* ed. Ch. Fehrenbach and B.E. Westerlund, D. Reidel Publ. Co., Dordrecht, p. 3.

Kurtz, M.J. 1983, in *Statistical Methods in Astronomy,* ESA SP-201, p. 47.

Lauberts, A. and Valentijn, E.A. 1983, *The Messenger* **34,** 10.

Lindemann, E. and Hauck, B. 1973, *Astron. Astrophys. Suppl.* **11,** 119.

Malinvaud, E. and Deville, J.C. 1983, *J. Roy. Statist. Soc.* A 146, 335–361.

Mersch, G. and Heck, A. 1980 *Astron. Astrophys.* **85,** 93.

Morgan, W.W. 1984, in *The MK Process and Stellar Classification,* ed. R.F. Garrison, David Dunlap Obs., p. 18.

Murtagh, F. and Lauberts, A. 1985, Comm. to Fourth Meeting of Classification Societies, Cambridge.

Narlikar, J.V. 1982, Indian J. Statist. 44, 125.

Strömgren, B. 1966, *Ann. Rev. Astron. Astrophys.* **4,** 433.

Strömgren, B. 1967, in *The Magnetic and Related Stars,* ed. R. Cameron, Mono Book Corp., Baltimore, p. 461.

Thonnat, M. 1985, INRIA (Centre Sophia Antipolis) Report No. 387.

NEWS ON ESO INSTRUMENTATION

The following information on instrumentation has been provided by the Optical Instrumentation Group.

The ESO Multiple Object Spectroscopic Facility "OPTOPUS"

OPTOPUS is a fiber-optics instrument intended for multiple-object spectroscopy with the Boller & Chivens spectrograph and a CCD detector at the 3.6 m telescope. Using the Optopus system, the spectra from up to 47 independent objects located within a 33 arcmin field can be simultaneously recorded.

Overall View of the System

For multi-object observations, the B & C spectrograph is mounted on a separate frame within the Cassegrain cage of the 3.6 m telescope and a special fiber optics adaptor is fixed to the Cassegrain flange. The adaptor serves as a support for metal templates (starplates) containing precisely drilled holes (corresponding to the objects of interest for a given observed field) into which the individual fibers are connected. The fibers, serving the purpose of a flexible light transport from focal plane to spectrograph, are terminated together at their output ends in a closely packed row which replaces the conventional B & C entrance slit.

For guiding and alignment purposes, each starplate must also contain bundle connector holes for two guidestars, which

are then observed from the control room by means of coherent fiber bundles and a TV camera mounted on the Optopus adaptor.

The usual B & C off-axis F/8 collimating mirror is replaced by an F/3 dioptric collimator to improve the efficiency of the system. On the RCA CCD detector, a single fiber is matched to 2.1 pixels and the individual spectra are separated by 4 pixel-high unexposed bands. The choice of grating determines the spectral coverage and resolution, exactly as in conventional use of the B & C spectrograph. One must consider that the resolution limit (determined by the fiber core diameter instead of a chosen slit width) is between 2 and 3 pixels, and that the length of the CCD in the direction of dispersion is 15 mm (~500 pixels).

The efficiency of Optopus should be comparable to that of the spectrograph used in normal mode, with some losses introduced by fiber/object misalignments and by material absorption in the fibers. For an object with m_v = 18 it is expected that a S/N ≥ 10 can be achieved at 170 Å/mm after a one-hour exposure, using the present CCD. The efficiency of the system begins to drop sharply below 3900 Å due to a combination of poor UV transmission in the fibers and reduced blue quantum efficiency of the CCD.

Preparation of the Starplates

Starplates for Optopus observations are prepared in the ESO workshop in Garching, using computer generated drilling machine instructions recorded on cassette. This is achieved, starting with a suitable (α, δ) coordinate file which is processed by a dedicated interactive computer program (OCTOP). For this purpose, astronomers to whom Optopus observing time has been granted will be required to travel to Garching at least two months in advance of their observing run at La Silla. ESO will support this trip as an integral part of the observing program. If the astronomer does not have accurate coordinates for the objects he wishes to observe, he can use a measuring machine and the astrometric program at ESO on his own photographic plates (or on sky survey plates) to obtain the source file for OCTOP. An auxiliary plotting program supplies the astronomer with a correctly scaled and numbered map of each processed starplate field.

Summary of Physical Constants and Constraints for OPTOPUS Starplates

Field scale:	7.140 arcsec/mm
Maximum field:	274 mm (33 arcmin) diameter circular field
Fiber size on sky:	2.6 arcsec
Maximum number of objects:	47
Optimal coordinate precision:	0.2 arcsec (transmission losses are of the order of 5 % per 0.1 arcsec coordinate imprecision, for a seeing of 2 arcsec)
Number of guidestars:	2
Faintest guidestar magnitude:	16
Maximum magnitude difference for guidestars:	2.5
Minimum object-object separation:	3.4 mm (25 arcsec)
Minimum guidestar-object separation:	9 mm (64 arcsec)

The Limiting Capability of EFOSC

EFOSC, the ESO Faint Object Spectrograph and Camera has been described in the ESO Messenger No. 38, page 9. The operating manual will be available at the end of August. The first run of the instrument for visiting astronomers will take place in September.

In three test nights in March 1985, observations were performed to establish the limiting capability of the instrument. While the detailed results will be published elsewhere, we report here the values which can be helpful in planning the observing program.

In *direct imaging,* we analyzed a series of exposures in the V an B band of a selected area in the cluster W Cen.

With the present setup (CCD # 3) and a seeing giving stellar images of FWHM = 1.3 arcsec, we detected stars of m_v = 25 at S/N ≃ 3 in a 15-minute V exposure, the main source of noise being the statistical noise of the sky background. In this exposure, stars of m_v ≃ 17.5 saturate the CCD. A well-defined HR diagram has been obtained down to V magnitude ≃ 23.

In *slit spectroscopy,* several spectra of objects in the 20–22 V magnitude range were recorded at a dispersion of 230 Å/mm. With a slit of 1.5 arcsec, the resolution is ~15 Å. The S/N of the final spectra are between 5 and 10.

The *grism mode,* in which the dispersing element and possibly a filter are inserted in the optical beam of the spectrograph but no slit is used, should be a powerful tool to survey selected regions of the sky for different types of objects. We have used it only to search for QSO candidates in an area which had been looked at on a CFHT grens plate. At 900 Å/mm, the continuum of objects of m_v = 22 is well recorded in a 5-minute exposure. The best results were obtained when a B or a G Gunn filter were used to reduce the length of the spectra and the sky background. A cursory inspection of three EFOSC fields has led to the discovery of a new QSO with m_v ≃ 21 and z = 3.27.

The Multiple Object Spectroscopy (MOS) Mode of EFOSC

In MOS, the EFOSC standard slit is replaced by a number of holes or rectangular slitlets, each exactly positioned on an object. The apertures are punched in a starplate, each one producing a spectrum. Theoretically, as many as 30 objects can be recorded if they fall within the MOS field of view, which is 3.6′ × 4.5′. Figure 1 shows an image of a starfield (made with EFOSC in direct imaging), Figure 2 the multiple spectra that were obtained.

In order to prepare a starplate, one needs to know the positions of the objects to sub-arcsecond accuracy. The procedure that was developed at ESO totally relies on the imaging capabilities of EFOSC. First, a direct image is obtained where positions are measured using the on-line data reduction system (IHAP). A drill coordinate list is then produced and it is sent to a dedicated machine which punches the starplate. The whole procedure will be the astronomer's responsibility.

The finished starplates are mounted in the EFOSC aperture wheel by an ESO operator during the following day and, on the second night, aligned on the sky again using EFOSC in direct imaging. Two images of the starplate and the starfield are compared, using IHAP, and the telescope offset and field rotation necessary to minimize position errors are computed. About 15 minutes are necessary for the alignment.

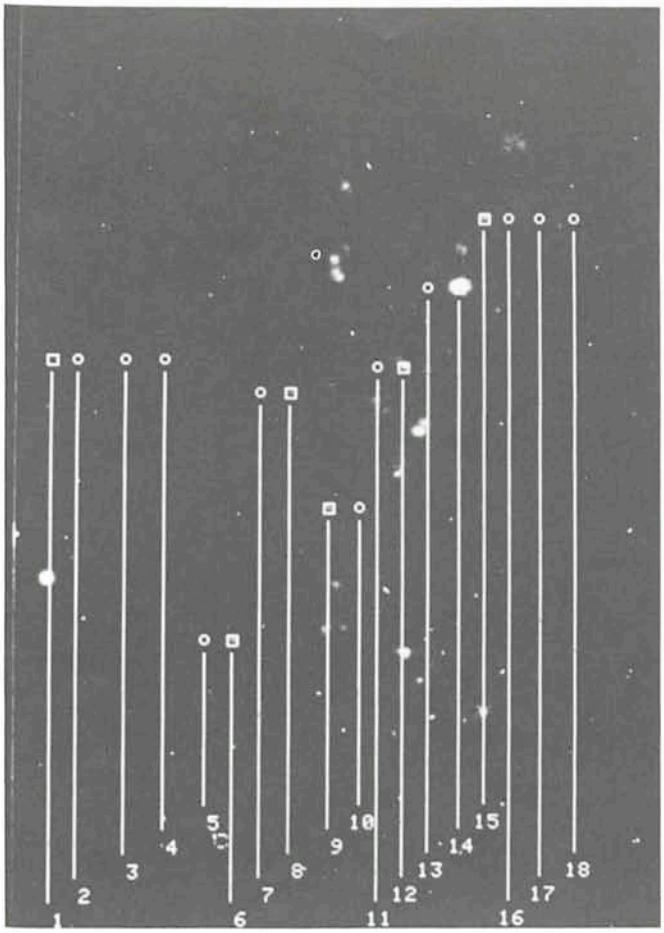

Figure 1: *This image shows HII regions in the spiral arms of M 83 with strong [OIII] emission. The overlayed, numbered boxes represent aperture requests for the punching machine: square boxes represent object holes, the round ones are sky holes. The image was obtained by subtracting an exposure taken through a narrow filter on the continuum from one centered on the emission line.*

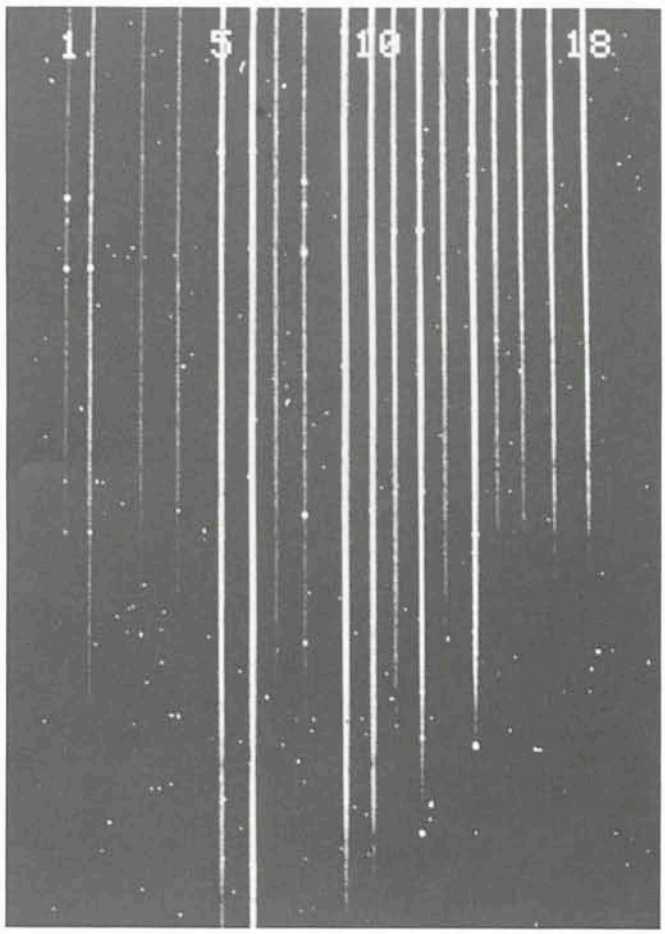

Figure 2: *The multiple spectra that were obtained from the aperture plate prepared from the image shown in Figure 1. The dispersion is 130 Å/mm and the wavelength coverage λλ 3700–5400 Å. The exposure time was 30 minutes. Point-like spots are radiation events on the CCD. The spectra are numbered as the apertures in Figure 1.*

The punching machine is being built in the framework of a collaboration between ESO and the Observatoire du Pic du Midi et de Toulouse; it will be tested at the telescope next February. MOS as described here will be offered for general use as of April 1986.

A New Short Camera at the CES

This new, faster camera is a dioptric system with aperture 2.5.

It is foreseen to use it with an RCA SID 503 CCD, with 640 × 1024 pixels, 15 μm square in size. Typical features of this new camera-detector combination are:

- linear dispersion 2.7 Å/mm at 5000 Å,
- resolution with 1.2 arcsec slit about 60,000,
- spectral coverage in one CCD exposure 42 Å.

The gain with respect to the present MAKSUTOV Camera (Long Camera) + Reticon combination should be of 1.5–2 magnitudes at comparable resolution in the blue-visual region. The actual value will depend on the quantum efficiency and read-out-noise of the CCD, which are now being measured.

The first tests at the telescope are foreseen in December 1985.

CCDs in Use at La Silla

There are at present four CCDs in operation at different telescopes and instruments at La Silla. Three are from RCA and one is a GEC coated in the ESO detector laboratory with a fluorescent plastic film to enhance the UV quantum efficiency. The table summarizes their basic parameters and performance. Some of these values could be slightly different during your actual observing run.

The format of the RCA CCD is 320 × 512 pixels, 30 μm square in size. The GEC is 385 × 576 pixels, 22 μm square in size. The responsive quantum efficiencies of the RCA # 5 and of the coated GEC CCD are shown in the figure. The RCA # 3

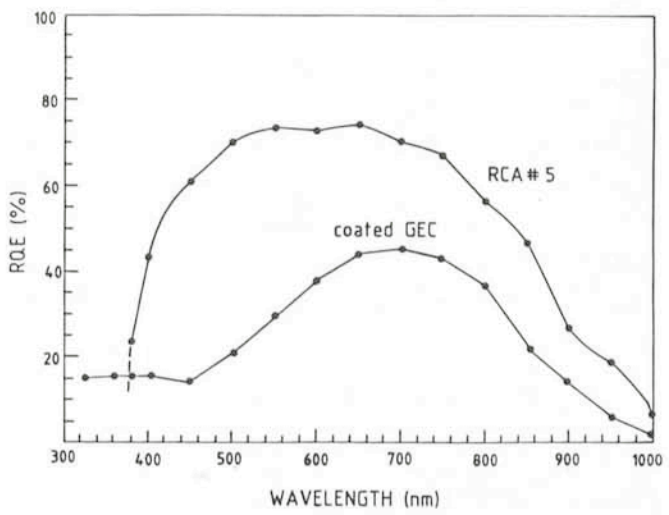

ESO, the European Southern Observatory, was created in 1962 to . . . establish and operate an astronomical observatory in the southern hemisphere, equipped with powerful instruments, with the aim of furthering and organizing collaboration in astronomy . . . It is supported by eight countries: Belgium, Denmark, France, the Federal Republic of Germany, Italy, the Netherlands, Sweden and Switzerland. It operates the La Silla observatory in the Atacama desert, 600 km north of Santiago de Chile, at 2,400 m altitude, where thirteen telescopes with apertures up to 3.6 m are presently in operation. The astronomical observations on La Silla are carried out by visiting astronomers – mainly from the member countries – and, to some extent, by ESO staff astronomers, often in collaboration with the former. The ESO Headquarters in Europe are located in Garching, near Munich. ESO has about 135 international staff members in Europe and Chile and about 120 local staff members in Santiago and on La Silla. In addition, there are a number of fellows and scientific associates.

The ESO MESSENGER is published four times a year: in March, June, September and December. It is distributed free to ESO personnel and others interested in astronomy.

Technical editor: Kurt Kjär

EUROPEAN
SOUTHERN OBSERVATORY
Karl-Schwarzschild-Str. 2
D-8046 Garching b. München
Fed. Rep. of Germany
Tel. (089) 32006-0
Telex 5-28282-0 eo d
Telefax: (089) 3202362

Printed by Universitätsdruckerei
Dr. C. Wolf & Sohn
Heidemannstraße 166
8000 München 45
Fed. Rep. of Germany

ISSN 0722-6691

Dewar #	1	3	6	5
Telescope	Danish 1.54 m	3.6 m	3.6 m / 2.2 m	2.2 m
Chip type	RCA SID 53612	RCA SID 501 EX	GEC P8603/A Fluor. coated	RCA SID 501 EX
e^-/ADU and gain*	18 at G50	11 at G50	8.5 at G100	11 at G30
Read out noise (e^-)	85	45	28	45
Charge transfer efficiency	150 ADU of background needed	Generally no charge smearing	~100 ADU of background needed	Generally no charge smearing
Blemishes	Some hot spots and 1 poor column	one hot column	A few partly dead columns	1 hot column, a hot spot at the on chip amplifier

has a behaviour similar to #5. The curve of RCA #1 has not been measured in detail. With respect to the other two it has a somewhat lower peak efficiency in the visual-red region but a better sensitivity in the UV region.

The saturation level of all of the CCDs is at present determined by the digital-analog-converter. This being limited to 16,000 ADU, saturation occurs for a number of electrons which depends on the operating gain.

In period 37, two new CCDs should be in operation. One is a RCA type SID 503 with 640 × 1024 pixels, 15 μm in size. It is going to be dedicated to the short camera of the CES and it is currently being tested. An additional coated GEC should also be available with the 2.2 and 3.6 m instruments.

Note, finally, that the present distribution of CCDs might be subject to changes if this is judged necessary by the ESO Directorate.

El Cometa Halley observado desde La Silla

Mientras el periódico cometa Halley se acerca rápidamente al sol, se están haciendo preparativos en muchos lugares para observar este distinguido objeto celeste. Durante la mayor parte de los meses junio y julio de 1985 Halley se encontraba "detrás" del sol y no podía ser observado. Desde aproximadamente el 18 de julio se intentó tomar imágenes de Halley en varios lugares y quedó verificado ahora que las primeras visiones confirmadas fueron hechas desde el Observatorio Europeo Austral el día 19 de julio.

En esa fecha Halley se encontraba en la declinación +18 grados y sólo a 30 grados al oeste del sol. El único telescopio en La Silla capaz de apuntar en esa dirección es el astrógrafo doble de 40 cm (GPO), el telescopio más pequeño en La Silla; y se dudaba del resultado obtenido del intento de observar Halley, durante el cual habíamos logrado obtener tan solo una placa en esa mañana. Una vez procesada, la placa fue inspeccionada muy cuidadosamente – mostraba estrellas de magnitud 16 y aun mas débiles, pero no se registraba una clara imágen del cometa.

Después de mi regreso a ESO Garching hacia fines de julio, el fotógrafo de ESO K. Madsen, y yo decidimos estudiar las placas más detalladamente. Se confeccionó una copia de la placa ampliada fotográficamente (este método permite ver mejor los objetos muy débiles y lejanos) y la placa fue medida en el instrumento de medición S-3000. Y verdaderamente se podía divisar un objeto muy débil y difuso cerca de la posición esperada. No correspondía a ninguna imágen del Atlas de Palomar. Aunque difícil de medir, se pudo transmitir una posición al Dr. Marsden de la Oficina de Telegramas Central de la Unión Astronómica Internacional.

Aunque este hecho no tiene un gran valor científico, encierra buenas perspectivas para las observaciones de ESO del cometa Halley a mediados de febrero de 1986, cuando éste reaparezca detrás del sol. Entonces nuestras observaciones serán bastante más importantes porque contribuirán esencialmente a la navegación de las aeronaves espaciales que están ya en camino hacia Halley para encuentros cercanos. Y naturalmente, siempre es agradable ser el primero, al menos de vez en cuando . . .!

R. WEST

Contents